AD-A109 605 FLORIDA STATE UNIV TALLAHASSEE DEPT OF OCEANOGRAPHY F/G 8/3
VARIABILITY OF THE ANTICYCLONIC CIRCULATION IN THE WESTERN GULF--ETC(U)
SEP 81 R D KASSLER, W STURGES N00014-75-C-0201
UNCLASSIFIED 189 NL

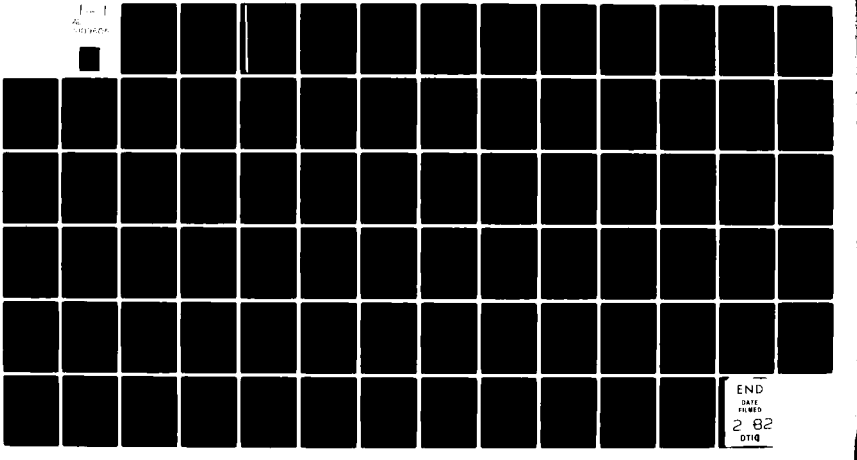

END
DATE FILMED
2 82
DTIC

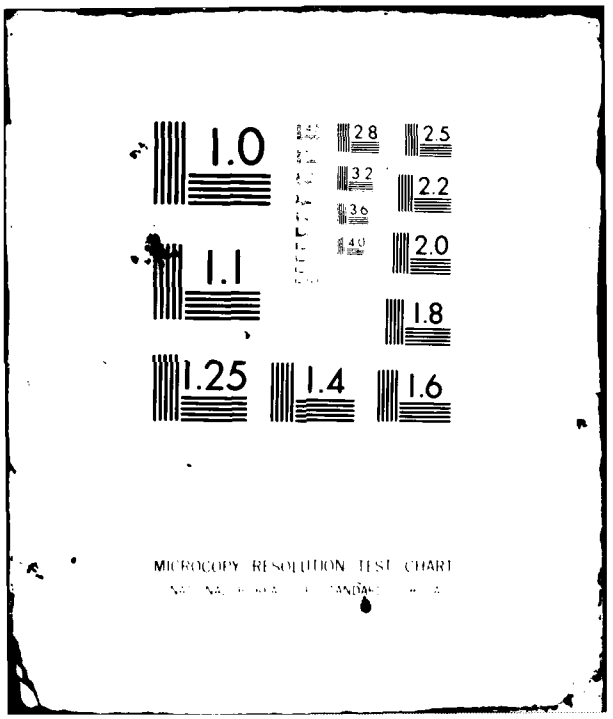
1.0
1.1
1.25
1.4
1.6
1.8
2.0
2.2
2.5
2.8
3.2
3.6
4.0
MICROCOPY RESOLUTION TEST CHART

SECURITY CLASSIFICATION OF THIS PAGE (When Data Entered)

REPORT DOCUMENTATION PAGE

READ INSTRUCTIONS BEFORE COMPLETING FORM

1. REPORT NUMBER: 189	2. GOVT ACCESSION NO.: AD A109605
3. RECIPIENT'S CATALOG NUMBER:	
4. TITLE (and Subtitle): Variability of the Anticylonic Circulation in the Western Gulf of Mexico	5. TYPE OF REPORT & PERIOD COVERED: Technical Report
	6. PERFORMING ORG. REPORT NUMBER:
7. AUTHOR(s): Richard D. Kassler and Wilton Sturges	8. CONTRACT OR GRANT NUMBER(s): N00014-75-C-0201
9. PERFORMING ORGANIZATION NAME AND ADDRESS: Department of Oceanography, Florida State University, Tallahassee, Fl 32306	10. PROGRAM ELEMENT, PROJECT, TASK AREA & WORK UNIT NUMBERS: NR-083-231
11. CONTROLLING OFFICE NAME AND ADDRESS: Office of Naval Research, NORDA, Tallahassee, Fl 32306	12. REPORT DATE: September, 1981
	13. NUMBER OF PAGES: 75
14. MONITORING AGENCY NAME & ADDRESS (if different from Controlling Office)	15. SECURITY CLASS. (of this report)
	15a. DECLASSIFICATION/DOWNGRADING SCHEDULE

LEVEL II

16. DISTRIBUTION STATEMENT (of this report)

Approved for public release; distribution unlimited

JAN 15 1982

17. DISTRIBUTION STATEMENT (of the abstract entered in Block 20, if different from Report)

18. SUPPLEMENTARY NOTES

A Florida State University Department of Oceanography Technical Report

19. KEY WORDS (Continue on reverse side if necessary and identify by block number)

20. ABSTRACT (Continue on reverse side if necessary and identify by block number)

The anticyclonic circulation in the western Gulf of Mexico is studied through 6 AXBT flights, 5 cruises, and moored current meter data over the course of a year, as well as through examination of the historical data base. It is concluded that the flow field consists of: a background circulation presumably forced by the curl of the wind stress; and the presence of warm core rings which periodically pinch off from the Loop Current.

All available meteorological data shows that negative curl dominates the

DD FORM 1 JAN 73 1473 EDITION OF 1 NOV 65 IS OBSOLETE
S/N 0102-014-6601

SECURITY CLASSIFICATION OF THIS PAGE (When Data Entered)

the central and western Gulf basin throughout the year. The Sverdrup relation gives a mean interior southerly transport of 5.6 x $10^6 m^3 s^{-1}$; a geostrphic calculation relative to 1500 m yields 8.5 x 10^6 m^3 s^{-1} to the south. Geostrophic transports relative to 1500 m across the western boundary current are on the order of 10 x 10^6 m^3 s^{-1}.

A time average of the mean flow field is formed over the passage of two large rings. The fluctuations in the rings have energy peaking at six month periods and wavelengths of ~430 km. When ring energy reaches the western boundary, some of the energy is reflected at wavelengths of ~80 km, while some is advected north by the mean flow and some propagates south along the continental rise.

THE FLORIDA STATE UNIVERSITY

DEPARTMENT OF OCEANOGRAPHY

VARIABILITY OF THE ANTICYCLONIC CIRCULATION IN THE WESTERN GULF OF MEXICO

Technical Report

Richard D. Kassler

and

Wilton Sturges

A Progress Report under ONR Contract N00014-75-C-0201

September 1981

12

THE FLORIDA STATE UNIVERSITY

DEPARTMENT OF OCEANOGRAPHY

VARIABILITY OF THE ANTICYCLONIC CIRCULATION IN THE WESTERN GULF OF MEXICO

Technical Report

Richard D. Kassler

and

Wilton Sturges

A Progress Report under ONR Contract N00014-75-C-0201

September 1981

TABLE OF CONTENTS

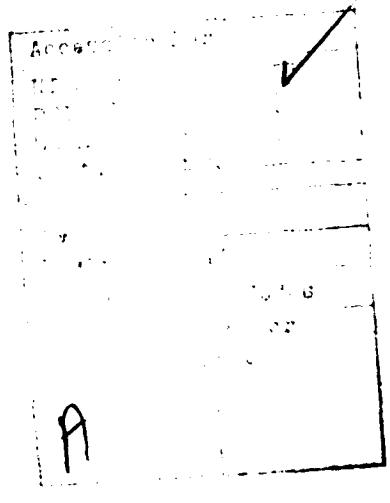

INTRODUCTION

The objective of this study is to gain a better understanding of the anticyclonic gyre in the western Gulf of Mexico, and, consequently, to examine the hypothesis that wind stress curl forcing drives the gyre and an associated western boundary current in a manner analogous to the North Atlantic Gulf Stream system (Sturges and Blaha, 1976). It has also been suggested that the gyre is maintained by anticyclonic rings which periodically pinch off from the Loop Current in the eastern Gulf and translate westward across the basin (*Ichye, 1962*; *Cochrane*, 1972; Nowlin and Hubertz, 1972; Elliott, 1981). Nowlin and McLellan (1967; also Nowlin, 1972) present a contour of the dynamic topography of the sea surface relative to the 1000-db surface for the entire Gulf of Mexico (Figure A-1, Appendix A). The dominant feature in the eastern Gulf is the Loop Current (see also Behringer et. al., 1977; Vukovich et. al., 1979), while the dominant feature in the west is the anticyclonic gyre (also shown by Behringer et. al., 1977; Merrell and Morrison, 1981).

The persistence of the western gyre is well documented in the literature. Nowlin (1972) presents a composite plot of N - S sections of geopotential anomalies from three different winters

(his Figure 1-38b). The data are similar, showing: an anticyclonic gyre centered at about 23.5°N, a region of more variability but lower geopotential north of the gyre, and a low in the Bay of Campeche. Behringer et. al. (1977) analyze average monthly temperatures at 200 m and find a large area of warm water located near 24°N in those months when the data is sufficient. This is consistent with an anticyclonic circulation, the persistence of which from month to month is evidence for a permanent anticyclonic gyre. They find the feature most well defined in summer and winter and somewhat fragmented in spring and fall, their Figures 2 - 13. Merrell and Morrison (1981) find the anticyclonic gyre centered near 23°-30'N, 95°-50'W in April, 1978, and also find a cyclonic gyre to the north near 25°-20'N, 95°-20'W. This instantaneous survey generally agrees with the mean historical data discussed above.

Elliott (1981) reviews historical data and finds that the separation from the Loop Current and subsequent westward translation of warm core rings is not an uncommon occurrence. A descriptive study by Behringer et. al. (1977) suggests rings separate at periods of 8 - 17 months, with separations at periods of less than one year outnumbering separations at periods of greater than one year by 2:1. Hurlburt and Thompson (1980), using a non-linear two layer numerical model, find ring separation to be independent of annual forcing and highly variable, with a mean period of 9 - 10 months. Rings which translate into the western Gulf add complexity

to the data collected there. The dynamic height map from Nowlin and McLellan (1967; and Nowlin, 1972) implies that the signal in a ring is greater than that in the western gyre. Thus, a good time series of observations is needed in order to extract the mean. A data collection program which includes AXBT flights, hydrographic cruises, and current meter moorings was undertaken in the western Gulf.

This paper discusses that data from the present program which is currently available for analysis and also examines relevant historical data. The possibility of wind stress curl forcing is addressed. The present data set is analyzed synoptically and quantitatively. The influence of two warm core rings (which pinch off from the Loop Current and drift westward) upon the background ocean circulation in the western Gulf is discussed.

II. THE WIND STRESS CURL HYPOTHESIS

A. Wind Stress Curl Forcing

Sturges and Blaha (1976) hypothesize that wind stress curl, through linear Sverdrup dynamics, forces an interior southerly geostrophic flow and the associated western boundary current. In support of this hypothesis, Blaha and Sturges (1981) find coherence between wind stress curl in the west central Gulf and sea level all along the western boundary of the Gulf "which suggests dynamics not typical of locally driven shelf circulation" but rather of remote curl forcing. Their results also suggest an almost immediate response of the basin to changes in wind stress curl; coastal sea level along the western boundary lags curl by approximately one month.

Negative wind stress curl is one prerequisite for the expected dynamics. Sturges and Blaha (1976), using Hellerman's (1967) data, find negative curl dominates the basin interior December - February and June - August, while curl vanishes during spring and fall. Blaha and Sturges (1981) using a National Marine Fisheries Service data set, find negative curl dominating the central western Gulf throughout the year, with maximum values and areal extent in summer and winter and minimum in spring and fall, their Figure 7. They

also point out that Krishnamurti and Krishnamurti (1979) compute (using hourly satellite observations of low level cloud winds) an average negative wind stress curl across the central basin for the period 16 June - 23 August, 1974, during the Gate experiment. The Hastenrath and Lamb (1977) atlas shows negative curl dominating the basin throughout the year, with maximum areal extent in summer and winter and minumum in spring and fall. This atlas uses all available data from the period 1911 - 1970 (see Figure A-2, Appendix A). These values of negative curl, which are on the order of 1×10^{-8} dynes cm^{-3} are of the same order of magnitude as those observed in the North Atlantic at mid-latitudes (Stommel, 1964).

Emery and Csanady (1973) suggest that wind stress curl is responsible for the predominantly cyclonic circulation of Northern Hemisphere large lakes and inland seas (which have length scales on the order of 100 km). Thus, it is reasonable to expect that a basin the size of the Gulf (the deep basin, depths of about 2000 m or greater, extends approximately 1200 km east - west and 500 km north - south (see Figure A-3, Appendix A), responds to wind stress curl forcing.

The mean annual interior transport may be calculated using the linear Sverdrup relation:

$$\text{N - S mass transport } \overrightarrow{M^y} = \frac{\text{curl}_z \vec{\tau}^{\eta}}{\beta}$$

where $\beta \equiv$ variation of the Coriolis parameter with latitude $= 2 \times 10^{-13}\ cm^{-1}\ s^{-1}$

$\text{curl}_z \vec{\tau}^{\eta}$ ≡ vertical component of the curl of the surface wind stress = -1.6×10^{-8} dynes cm^{-3} (mean annual value for west central Gulf, from Blaha and Sturges, 1981)

$\vec{M}^{y} = 8 \times 10^{4}$ g cm^{-1} s^{-1} to the south

then N - S volume transport $\vec{V}^{y} = \vec{M}^{y} L \alpha$

where L ≡ applicable E - W basin extent = 700 km (it is shown later that this is reasonable)

α ≡ specific volume of sea water ≅ 1 cm^3 g^{-1}

$\vec{V}^{y} = 5.6 \times 10^{6}$ m^3 s^{-1} to the south.

Geostrophic transports relative to 1500 m across the western boundary current are computed to be:

11×10^{6} m^3 s^{-1} in July, 1979

10×10^{6} m^3 s^{-1} in November, 1979

27×10^{6} m^3 s^{-1} in July, 1980.

This suggestes the western boundary current returns all of the interior flow. (Geostrophic transports are discussed in more detail in a later section.)

Molinari (1978), using a numerical model for a steady, linear, quasi-geostrophic two layer ocean (which reduces to Stommel's 1948 model), finds that wind stress curl establishes a gyre in the western Gulf with balances in the interior between β and wind stress curl and in the western boundary current between lateral friction and curl. There is a caveat, however, in assuming a Sverdrup interior; the effects of mesoscale eddies (e.g. Rossby waves, rings) can

negate the validity of the linear approximation. Harrison (1979) suggests that the effects of eddies with horizontal length and velocity scales of 100 km and 10 cm s^{-1}, respectively, can be comparable to the β term in the vorticity balance of the North Atlantic. Lindstrom et. al. (1980) determine absolute velocities in the western North Atlantic using the Beta spiral method over different depth ranges and find discrepancies between the results given by the 300 - 1000-db range and those given by the 1100 - 1800-db range. They attribute the discrepancies (a factor of two or more) to the effects of eddies. It is likewise possible that the linear Sverdrup calculation presented above may be in error by a factor of two or more.

The time dependent response may also be examined. Rhines (1977) derives the ratio:

$$\frac{\text{average kinetic energy associated with a Rossby wave}}{\text{average kinetic energy associated with time dependent Sverdrup flow}} = \left(\frac{\beta L T}{2}\right)^2 = R$$

L = length scale of forcing

T = time scale of forcing

Take forcing to be wind stress curl.

In Gulf: $\beta = 2 \times 10^{-13}$ cm^{-1} s^{-1}

$$L = \frac{500 \text{ km}}{2\pi} = 7.8 \times 10^{6} \text{ cm}$$

$$T = \frac{6 \text{ mos.}}{2\pi} = 2.5 \times 10^{6} \text{ s}$$

$$R = \frac{(2 \times 10^{-13}\ \text{cm}^{-1}\ \text{s}^{-1})(7.8 \times 10^{6}\ \text{cm})(2.5 \times 10^{6}\ \text{s})}{2}^{2}$$

$$R = 4$$

This suggests Sverdrup flow is slightly preferred to Rossby waves in the time varying response.

B. Interior Geostrophic Transport Calculation

An interior transport of $5.6 \times 10^{6}\ m^{3}\ s^{-1}$ to the south is computed using the Sverdrup relation. It is interesting to compare this value with the results of the independent calculation of interior geostrophic transport using historical hydrographic stations in the western and eastern Gulf, similar to what Leetmaa et. al. (1977) do in the North Atlantic. The determination of the appropriate hydrostations to use in such a calculation is non-trivial.

1. Western Gulf

As is shown later, the mean position of the center of the western gyre during the period July, 1979 - July, 1980, is approximately 24^{o}-10'N, 95^{o}-07'W. All historical hydrostations closest to this location are averaged over temperature and position. The T - S curve from the Hidalgo, 1962, Gulf survey (see Nowlin and McLellan, 1967; Nowlin, 1972) is used to provide the salinities. The effect of the seasonal heating cycle in the upper 100 m is removed, based upon the results of Blaha and Sturges (1978), in their Appendix B.

Thus, a characteristic hydrostation near the west Gulf gyre center is obtained at 23°-49'N (±5'), 95°-05'W (±9'). Ten hydrostations from eight different surveys were appropriately weighted where necessary to avoid temporal bias.

All historical hydrographic data (81 hydrostations from 9 surveys) along 95°W are used to obtain averages, by 1.5° latitude bands, of the depth of the 14°C isotherm. To maximize the number of observations entering each averaging calculation, a boxcar type averaging is employed in which averages for fifteen 2.5° latitude bands are calculated, beginning with the band 19.0°N - 21.5°N and advancing successive bands by 0.5° latitude increments. Observations are appropriately weighted where necessary to avoid temporal bias. This calculation (see Figure 1) suggests that, in the mean, the gyre extends from 21°-15'N to 25°-30'N, centered near 23°-45'N. This result generally agrees with the mean depths of the 14°C isotherm calculated for the period July, 1979 - July, 1980 (also shown in Figure 1).

2. Eastern Gulf

Two ways to obtain an average hydrostation in the eastern Gulf were apparent: average all available data; or, exercise some sort of pre-selection. The latter method was employed; care was taken to eliminate the effect of the presence of both the Loop Current and the rings which separate from the Loop Current. Maps of the sea surface topography relative to 1000-db and of the temperature

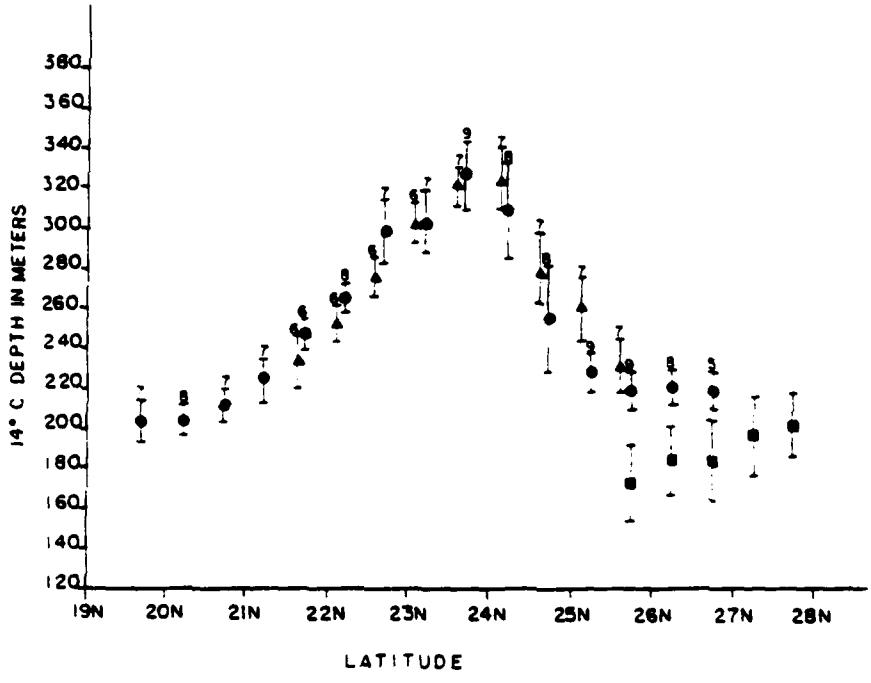

Figure 1. Mean depth of the 14°C isotherm in western and eastern Gulf of Mexico:
—●— from all NODC N - S hydrographic sections along 95°W, averaged over 1.5° latitude bands.
—▲— along 95°W, using the data from this study; see Figure 3.
—■— using hydrographic data in eastern Gulf, from five surveys representative of the background signal.
The number of surveys for —●— and —▲— is indicated above each data point.
Error bars are one standard deviation.

field at 150 m were studied (Molinari, 1980; his figures 8, and 10 - 13; see Figure A-4, Appendix A). As a result it was determined that hydrostations with temperatures of 16°C or less at 150 m were most likely situated in positions unaffected by Loop Current and ring presence. All available hydrostations satisfying this criterion were obtained and averaged over position and temperature. Thirty-two hydrostations from five different surveys were used. Observations were appropriately weighted where necessary to avoid temporal bias. Again, the effect of the seasonal heating cycle in the upper 100 m was removed. Since approximately 50% of the hydrostations were occupied by R.V. Alaminos, salinities were obtained from the Alaminos hydrostations' T - S curve.

The average position of the characteristic eastern hydrostation is 26°- 34'N (±16'), 89°-26'W (±38'). This position agrees well with the results of the Vukovich et. al. (1979) satellite analysis of Loop Current boundaries. Based upon an average of their Figures 2 (for the months of January - May, November, and December), this position lies in a region which is occupied by the Loop Current less than 25% of the time. A separation of 700 km is obtained between the characteristic eastern and western hydrostations.

The hydrographic data in the east is also used to obtain averages, by 1.5° latitude bands, of the depth of the 14°C isotherm. Again, boxcar type averaging is used and observations are weighted to avoid temporal bias. This calculation (see Figure 1) suggests a general decrease in thermocline depth of the background signal

with decreasing latitude in the eastern Gulf over the area where data was available (25^{o}N - 28^{o}-30'N).

3. Results

An interior southerly geostrophic transport relative to 1500 m of 19 X 10^{6} $m^{3}s^{-1}$ ± 40% results (with a calculated mean northward Ekman transport of 0.2 X 10^{6} m^{3} s^{-1} subtracted out, see Appendix B). The error bar is obtained by propagating the effects of one standard deviation of all values averaged (e.g. latitude, longitude, temperature) throughout the calculation. Figure 2 shows the velocity profile obtained. This is an unrealistic result. Mean southerly velocities on the order of 5 cm s^{-1} are not observed in the upper 200 m of the Gulf interior. Analysis of the procedure reveals that the data is biased toward greater transports by an inconsistency in the choice of the characteristic hydrostations. The characteristic western hydrostation includes the effects of rings, but the characteristic eastern hydrostation does not.

If the following are assumed: a characteristic ring signal (i.e. - a dynamic topography of the sea surface relative to 1000-db of 1.8 dynamic meters, from examination of Molinari, 1980, maps), a ring root mean square diameter of 370 km (from Elliott, 1981), a ring mean translation speed of 3 km/day (from Elliott, 1981), a ring mean separation period from the Loop Current of twelve months, and the influence of a ring then applied to the background signal of our characteristic eastern Gulf hydrostation; an interior southerly transport between the stations of 8.5 X 10^{6} m^{3} s^{-1} ± 40% is

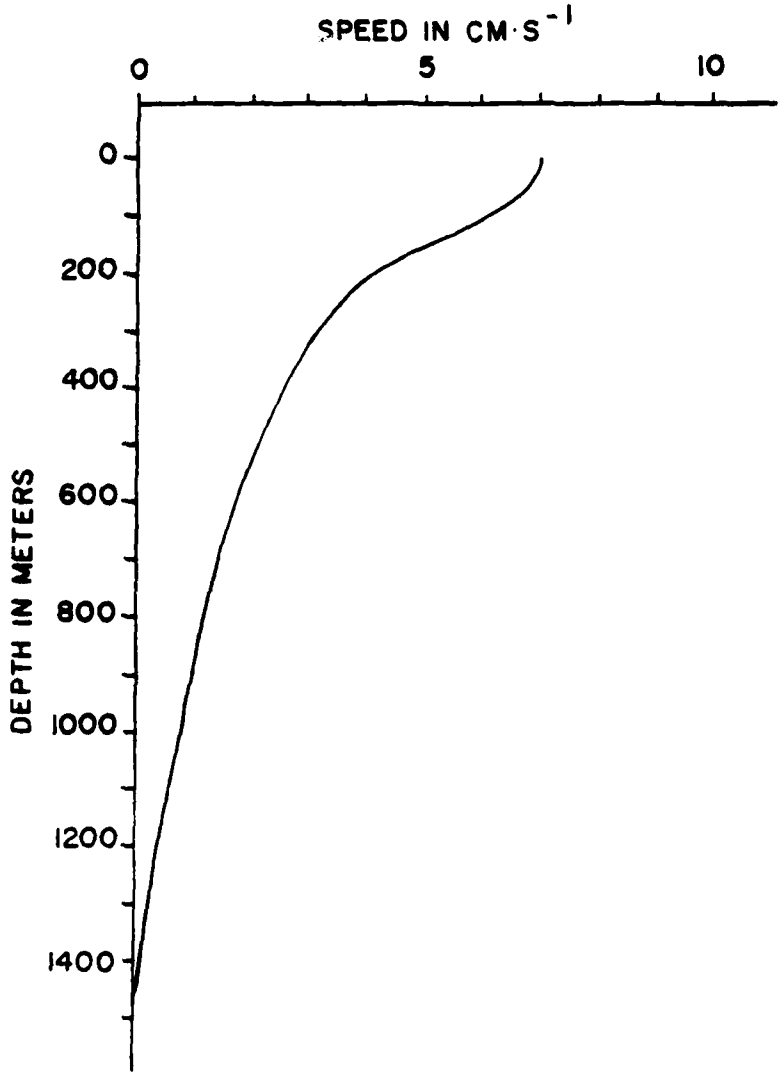

Figure 2. Geostrophic velocity versus depth relative to 1500 m obtained from the interior geostrophic calculation between 95°W and 89°-30'W.

estimated (see Appendix C). This agrees well with the 5.6×10^6 m^3 s^{-1} computed from the Sverdrup relation. In addition, the velocity profile shown in Figure 2 decreases in amplitude by a factor of more than two.

Much can be learned from these calculations. The first attempt suffers from an inconsistency in station choice. To do a better calculation, all available hydrostations in a region typically just west of the western edge of the Loop Current must be used. An important result is that it is possible to calculate, using hydrographic data, interior geostrophic flow to the south. The effect of rings dominates the background signal in the interior. The influence of a ring upon the background signal depends upon: ring amplitude, ring shape, ring radius, the ring separation time scale, and the local time scale of ring passage.

III. SYNOPTIC ANALYSIS AND HYDROGRAPHIC DATA SET

The data examined in this study were derived from five hydrographic cruises, a current meter array along 24°N, and six AXBT flights, Figure 3. AXBT surveys have been widely used by researchers during the past decade. One of the more ambitious of these has been the Hawaii/Tahiti Shuttle Experiment which consisted of 35 flights during which 1,893 AXBTs were launched, with a 94% success rate (Stroup et. al., 1981). During the present Gulf of Mexico experiment, 344 AXBTs were launched from U.S. Navy P-3 aircraft with a 95% success rate. Based upon contouring of the data, a subjective estimate of the reliability of an AXBT given depth of a mid-thermocline isotherm is 5 - 10 m.

Devising appropriate flight patterns proved to be a non-trivial task. Flight patterns were based upon a compromise of two conflicting requirements: the available on station flight time, which varied from six to eight hours; and an attempt to observe an ocean circulation based upon pre-conceived ideas of what it would look like, which changed as the experiment progressed. Once the AXBT data were processed and supplemented with the cruise data, a series of synoptic pictures of the depth of the 14°C isotherm in the western Gulf was contoured.

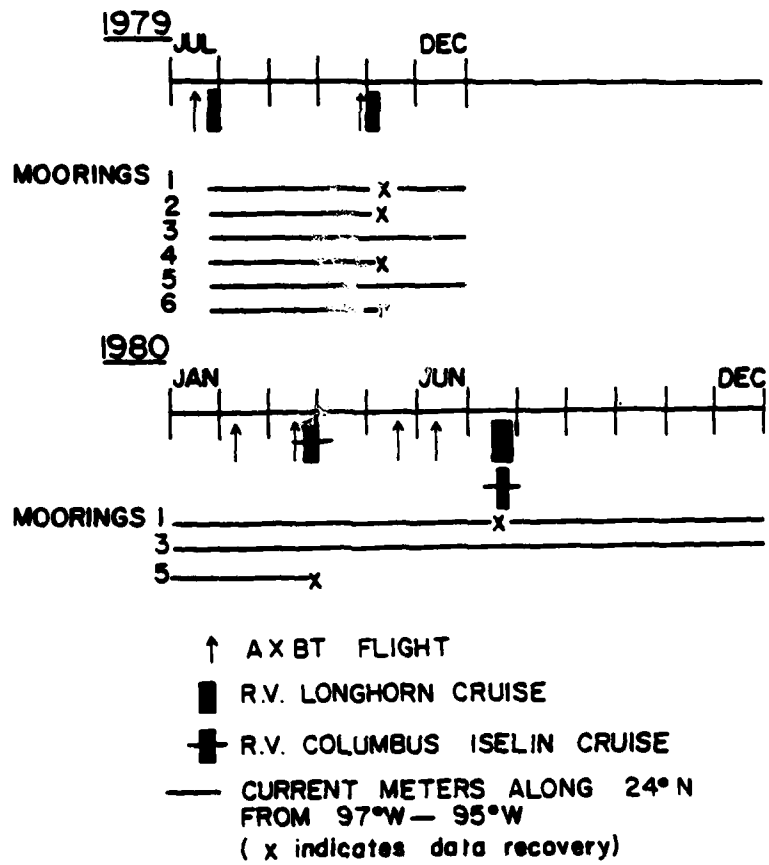

Figure 3. Time line showing origin of the 1979 - 1980 data set. Data from the July, 1980, R.V. Iselin cruise is provided courtesy of David Brooks.

A. Synoptic Maps

1. July, 1979; Figure 4 - A broad anticyclonic flow much like a classical wind stress curl driven gyre is evident. There is a negative side-lobe feature at about 22°N, 92°-30'W. Such features may be associated with the dispersion of rings, as shown by Flierl (1977) in a linear model and by McWilliams and Flierl (1979) in a non-linear model. Evidence does exist in support of the arrival of a ring in the western Gulf just prior to the July surveys. An XBT transect by USCGC Valiant extending on a line from 25°-28'N, 84°-03'W to 27°-44'N, 93°-10'W shows the presence of a high with a 300 km diameter centered near 26°-50'N, 90°-15'W on 25 February, 1979. This implies an average translation of 4.4 km/day at 245°T for this feature to arrive in the western Gulf by the end of June, 1979. The diameter of this feature and its inferred translation fall within the limits of historical observation of Gulf of Mexico rings (Elliott, 1981).

2. November, 1979; Figure 5 - The flow field seems quite fragmented and in this sense differs from the other synoptic maps. There is an anticyclonic gyre in the western Gulf of smaller spatial scale than in July. The feature centered at about 21°-30'N, 94°-30'W may be the negative side-lobe feature seen in July or a manifestation of the cyclonic circulation sometimes observed in the Bay of Campeche. The high feature at about 25°N, 91°W is most likely the Loop Current. NOAA - NESS - EPB weekly Gulf Stream satellite analyses for 7 - 9 October, and 1 - 7 November, 1979, suggest the Loop Current penetrated

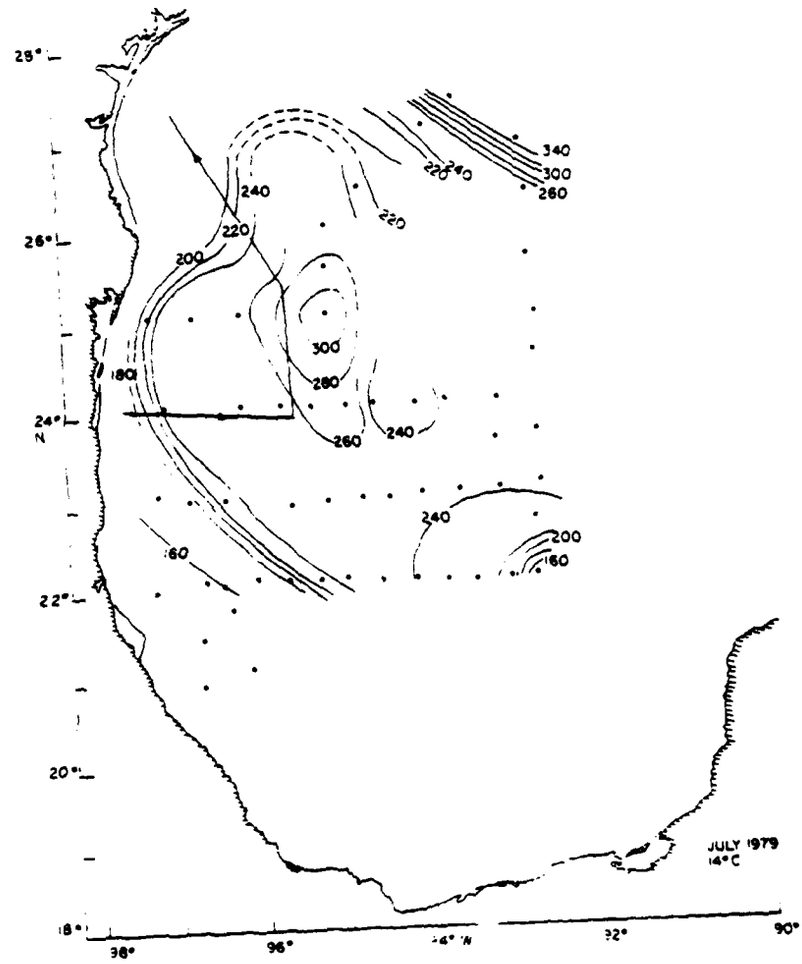

Figure 4. Depth of the 14°C isotherm in the western Gulf of Mexico from STD, XBT, and AXBT data, July, 1979. Dots show AXBT data points from 14 July; line shows trackline of R. V. Longhorn, 24 July - 1 August. Dashed contours represent some extrapolation. Depths are in meters.

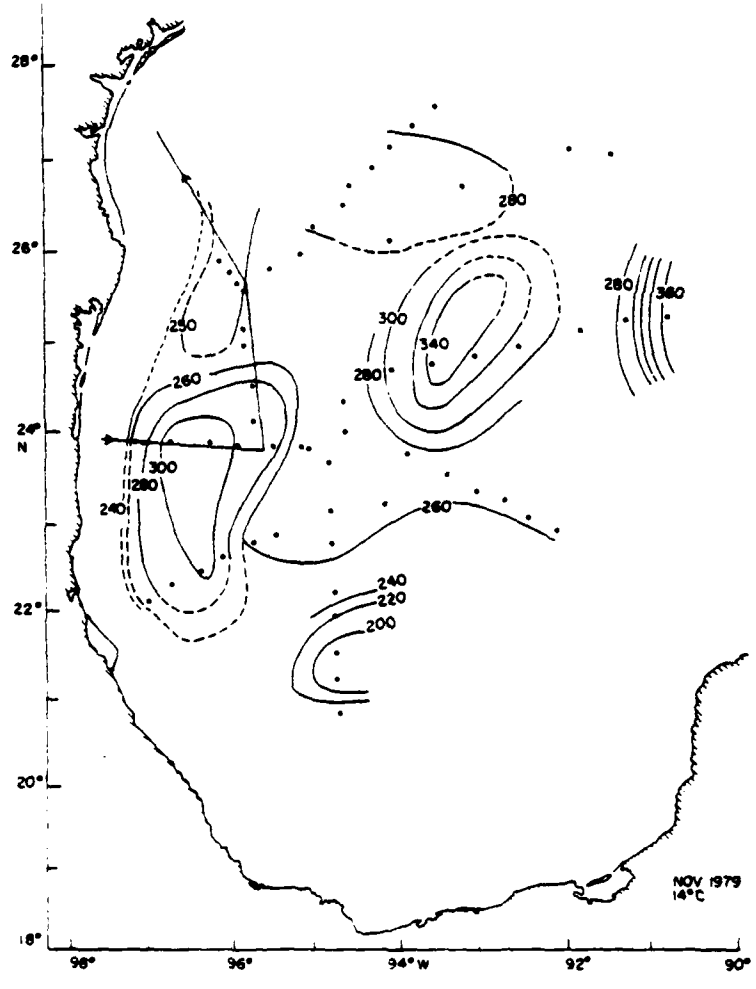

Figure 5. Depth of the 14°C isotherm in the western Gulf of Mexico from STD, XBT, and AXBT data, October and November, 1979. Dots show AXBT data points from 27 October; line shows trackline of R.V. Longhorn, 31 October - 6 November. Dashed contours represent some extrapolation. Depths are in meters.

well into the central Gulf during October and November. The high feature at about 25°N, 93°-30'W is more difficult to explain. It is unlikely that it derives from the Loop Current. If it does, a ring pinch off period of about four months between it and the ring which arrived just prior to July, 1979, is implied. Another explanation is that it is a ring which has recently pinched off from the western boundary current meandering offshore. A meandering and pinching-off process which occurred between July and November could possibly be the cause of the fragmented November flow field, but this is pure speculation. Meanders along the offshore trajectory of the western boundary current are not uncommon. A satellite IR picture of the western Gulf from 8 March, 1979, shows a meandering offshore flow east of Brownsville, Texas, which is reminiscent of the appearance of the Gulf Stream north of Cape Hatteras. Extensively meandering offshore flows are also evident in the March, May, and July, 1980, synoptic maps. The high feature may also be a manifestation of Rossby wave energy, but this is also speculation.

3. February, 1980; Figure 6 - The anticyclonic gyre is seen in the western Gulf. The high to the southeast of the gyre center may be the feature seen in November (at 25°N, 93°-30'W), had it translated at 1.4 km/day at 205°T, which seems easily possible. There is a weak cyclonic feature north of the anticyclone. This cyclonic circulation is also observed in April, 1978, by Merrell and Morrison (1981) and by Clemente-Colon (1980) in the fall of 1974 and in April, 1977. The feature is not well measured in this study since the main objective

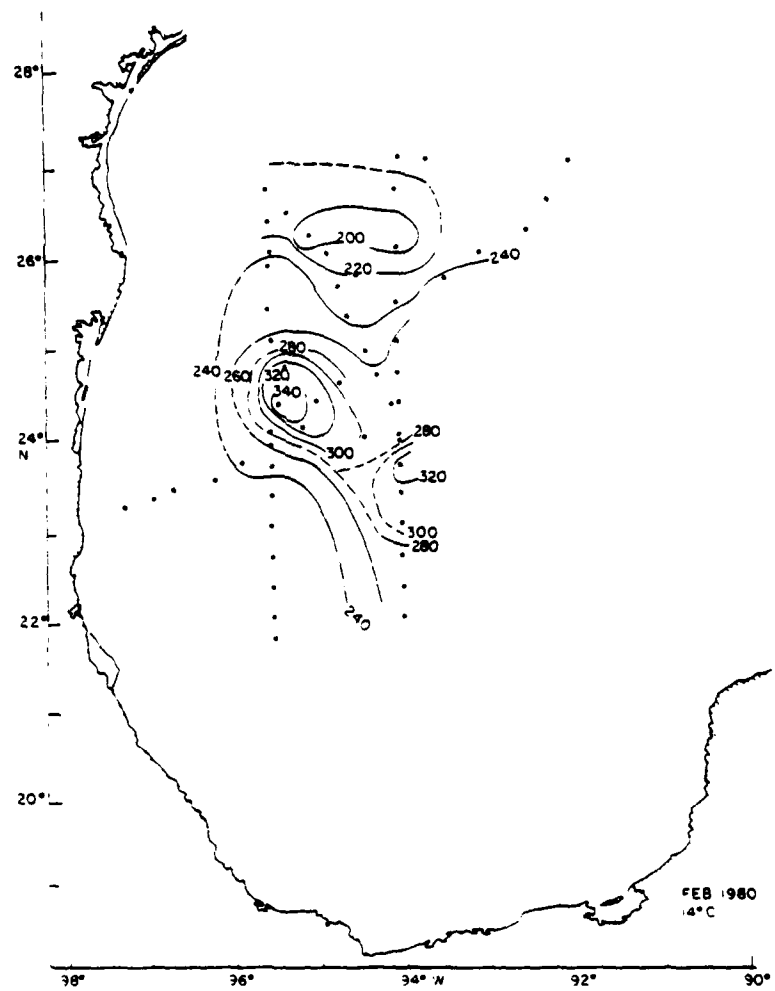

Figure 6. Depth of the 14°C isotherm in the western Gulf of Mexico from AXBT data, 9 February, 1980. Dots show AXBT data points. Dashed contours represent some extrapolation. Depths are in meters.

here is to learn more about the anticyclone.

4. March, 1980; Figure 7 - The anticyclonic gyre is seen in the western Gulf. A warm core anticyclonic ring, presumably recently separated from the Loop Current is the large feature seen centered on the map at 25°N, 91°-15'W (note that the center of the ring is most likely northeast of this position due to the apparent elliptical shape). NOAA - NESS - EPB weekly Gulf Stream satellite analyses indicate that the Loop Current retained its extended position in the central Gulf until January 1980, when a ring pinched off between 26 and 30 January. A negative side-lobe feature like the one seen in July is evident, centered at about 24°N, 90°-30'W, indicating that the ring has begun dispersing within sixty days of its formation.

5. May, 1980; Figure 8 - The anticyclonic gyre is seen in the western Gulf. The ring is now centered at 25°N, 92°-50'W, implying the ring translated at about 4 km/day somewhat south of west since March. The 360 m, 380 m, and 400 m contours seen in March are not evident on the May map; this may be an artifact of the sampling since there is a gap in data coverage between 24°N and 25°N. The southerly component of translation is consistent with what Flierl (1977) finds -- that an elliptical Gaussian ring originally oriented northeast to southwest in the northern hemisphere tends to translate to the west, but with a small southward drift. The ring not only translates between March and May, but also appears to precess. The negative side-lobe is not so evident as in March, but is not as well sampled.

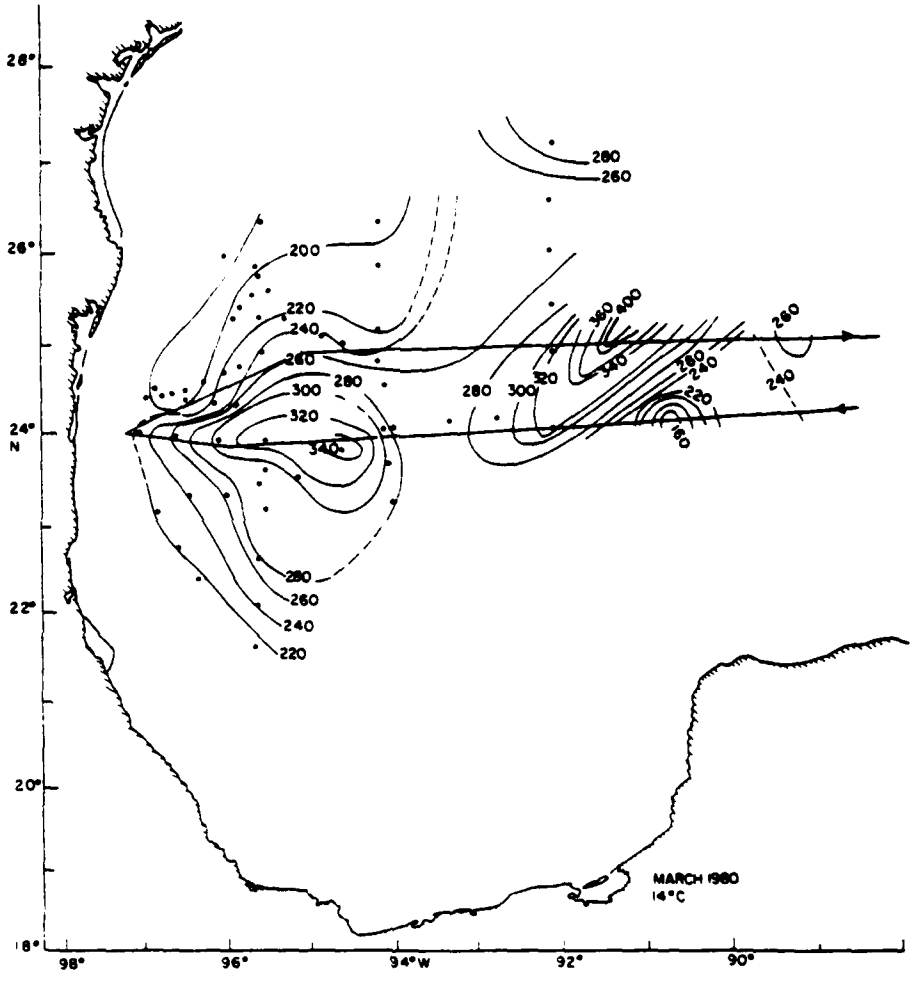

Figure 7. Depth of the 14°C isotherm in the western Gulf of Mexico from XBT and AXBT data, March, 1980. Dots show AXBT data points from 16 March; line shows trackline of R.V. Iselin, 24 - 29 March. Dashed contours represent some extrapolation. Depths are in meters.

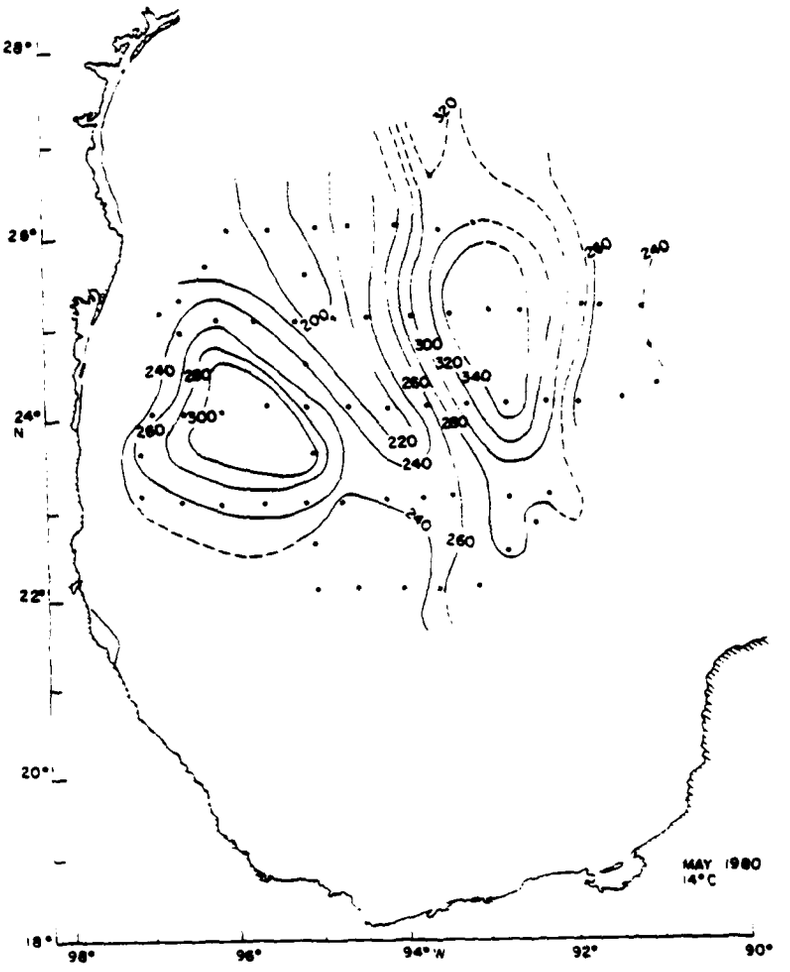

Figure 8. Depth of the 14°C isotherm in the western Gulf of Mexico from AXBT data, 17 May, 1980. Dots show AXBT data points. Dashed contours represent some extrapolation. Depths are in meters.

6. June, 1980; Figure 9 - The two anticyclonic features appear to have coalesced. Ring arrival seems to constructively reinforce the background circulation, implying the two features interact in a wave-like manner. The estimated geostrophic transports relative to 400 m across the western flanks of the gyre and the ring in May are 6×10^6 m^3 s^{-1} and 10×10^6 m^3 s^{-1}, respectively. The estimated geostrophic transport relative to 400 m across the eastern flank of the gyre in June is 15×10^6 m^3 s^{-1}. This suggests that the resultant feature obtains the sum of the transports. However, as is shown later, the error associated with the geostrophic calculations may be as high as ± 26%. There are indications of a negative side-lobe feature east of the gyre.

7. July, 1980; Figure 10 - The center of the western anticyclone has translated at about 5 km/day at 275°T from June - July. A large meander has developed along the gyre's northern flank. Some indications of a negative side-lobe are evident southeast of the gyre center.

8. Mean and Variability; Figure 11, Table 1A, Table 1B - The mean circulation in the central western Gulf during the period July, 1979 - July, 1980, is an anticyclonic gyre centered at approximately 24°-10'N, 95°-07'W, with N - S and E - W length scales of greater than 400 km and greater than 300 km, respectively. On the nearshore side of the gyre, the 14°C isotherm depth contours do not appear to close in the sense of a ring; the isotherm rises only 60 m, leaving the other 50% of the change to take place at larger scales. Tables 1A and 1B summarize the variability in the circulation during this period,

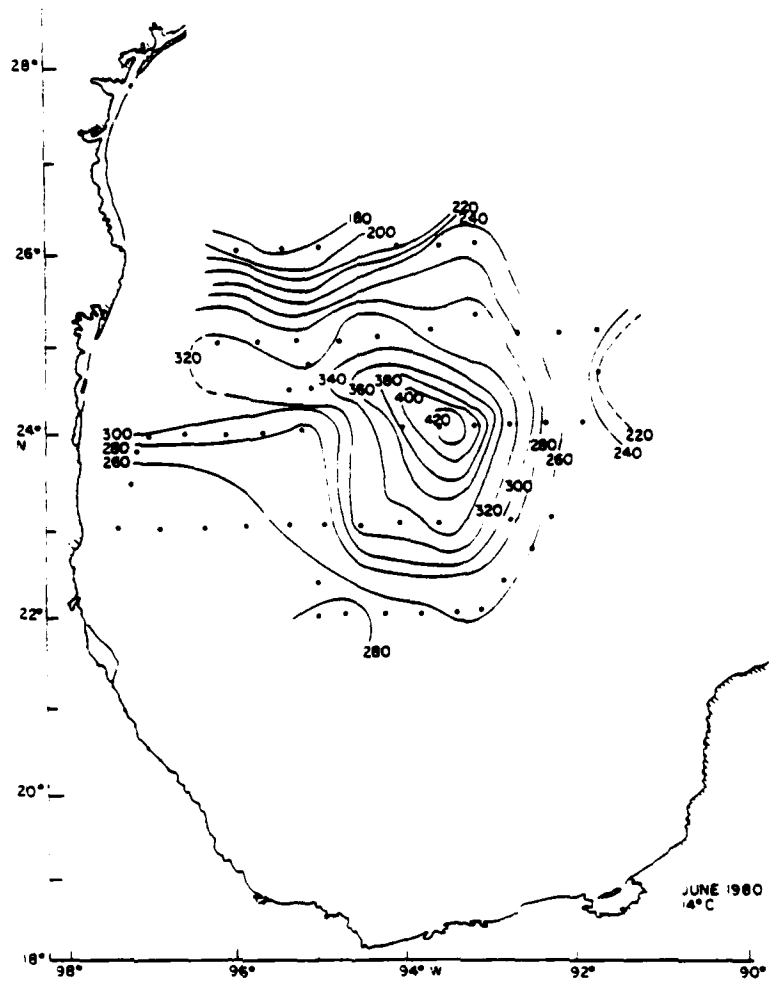

Figure 9. Depth of the 14°C isotherm in the western Gulf of Mexico from AXBT data, 12 June, 1980. Dots show AXBT data points. Dashed contours represent some extrapolation. Depths are in meters.

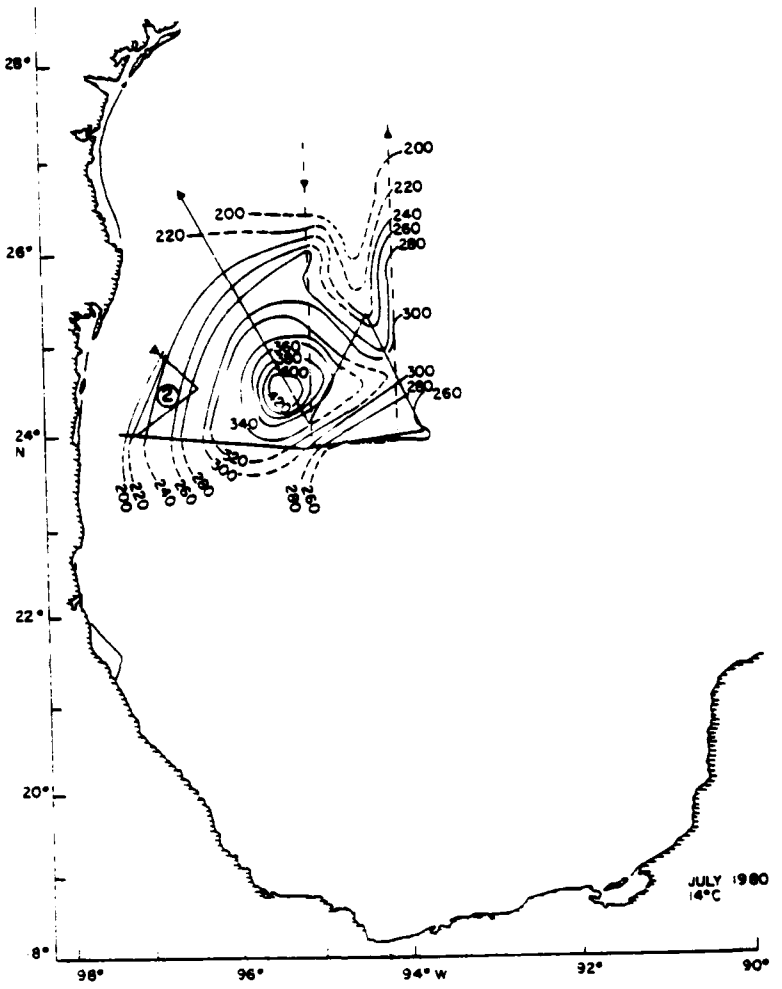

Figure 10. Depth of the 14°C isotherm in the western Gulf of Mexico from XBT and STD data, July, 1980. ——— shows trackline of R.V. Longhorn, 15 - 26 July. ——···——··· shows trackline of R.V. Iselin, 18 - 24 July (data courtesy of David Brooks). Dashed contours represent some extrapolation. Depths are in meters.

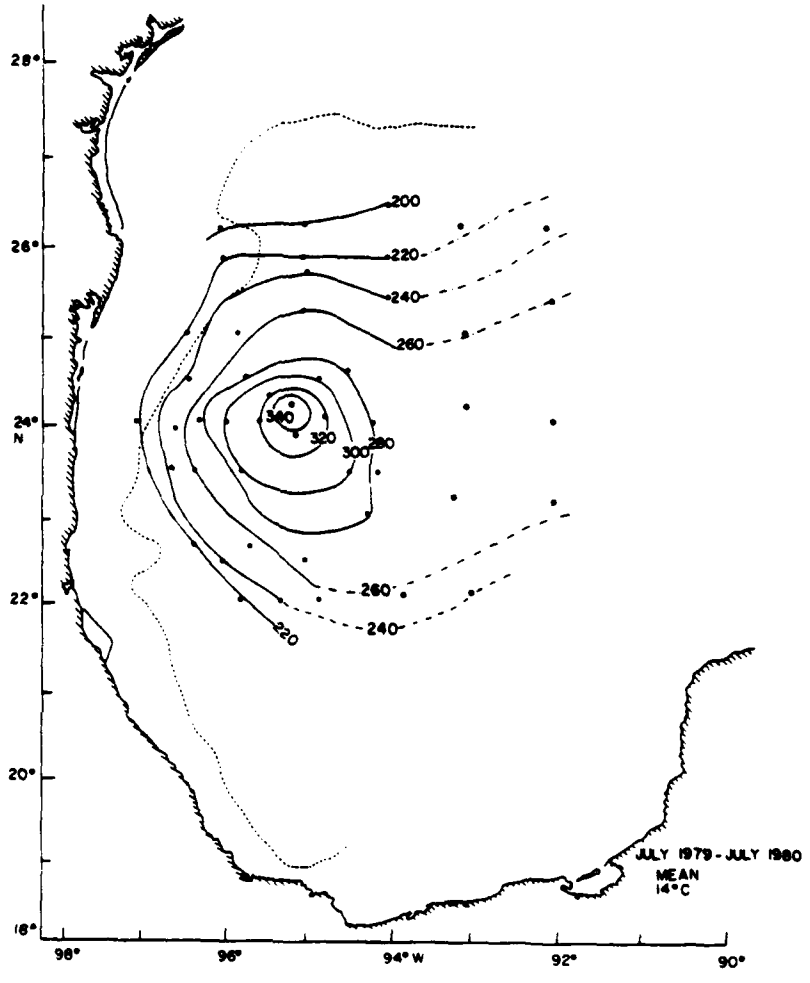

Figure 11. Mean depth of the 14°C isotherm in the western Gulf of Mexico, July, 1979 - July, 1980. Dots show positions where mean values are calculated. ----- represents the 1000 m isobath. —·—·— represents extension of contours into areas where mean values are derived from five observations or less. Depths are in meters.

MONTH	GYRE CENTER	N - S EXTENT (KM)	E - W EXTENT (KM)	CHANGE IN DEPTH OF 14°C ISOTHERM ACROSS SOUTH FLANK OF GYRE (M)	14°C ISOTHERM MAXIMUM DEPTH (M)
Jul 79	25-00N 95-00W	>600	370	91	310
Nov 79	23-50N 96-25W	330	220	79	313
Feb 80	24-22N 95-16W	280	200	117	357
Mar 80	23-45N 94-33W	400	330	132	351
May 80	23-55N 95-40W	350	270	85	319
Jun 80	24-00N 93-25W	450	500	170	430
Jul 80	24-17N 95-20W	>300	>300	182 (across north flank)	422
MEAN	24-10N ± 24' 95-07W ± 54'	>400	>300	122 ± 17	358 ± 20

Table 1A. Statistics for western gyre during the period July, 1979 - July, 1980. Error estimates are one standard deviation.

MONTH	RING CENTER	N - S EXTENT (KM)	E - W EXTENT (KM)	CHANGE IN DEPTH OF $14^{o}C$ ISOTHERM ACROSS SOUTH FLANK OF RING (M)	$14^{o}C$ ISOTHERM MAXIMUM DEPTH (M)
Mar 80	25-00N[1] 91-15W	---	---	123	403
May 80	25-00N 92-50W	400	330	79[2] (across west flank)	350[2]

1 As mentioned in text, the center of the March, 1980, ring is probably *northeast* of the area sampled.

2 That these May, 1980, values are significantly less than the March values is not necessarily an indication of the degree of ring dissipation; it may merely be a function of the sampling.

Table 1B. Statistics for warm core ring observed during the period July, 1979 - July, 1980. Error estimates are one standard deviation.

listing gyre and ring center positions, length scales, amplitudes, and 14°C isotherm maximum depths.

B. Geostrophic Transports and Velocities

1. Transports and velocities

Geostrophic transports relative to 400 m, 600 m and 1500 m across the western boundary current for July and November, 1979, and July, 1980, are listed in Table 2. Where necessary, hydrographic data is integrated up the bottom in order to include the edge of the current. Hydrographic data in July and November, 1979, is not consistently deep enough to permit reliable calculations below the 400 m and 600 m depths, respectively. Thus, this data is extrapolated to depth where appropriate, based upon comparison with historical hydrostations.

Transports in July and November, 1979, are comparable, with the exception of the transport across the northwest flank of the gyre in July. This difference may suggest that flow across the northwest flank in July, 1979, may be enhanced by offshore flow derived from the local shelf circulation. However, this is simply speculation, since, as is shown in the error analysis, this difference in transports lies within the noise level of the calculation.

Transports across the western and northwestern flanks in July, 1980, are almost three times those in July and November, 1979. The obvious reason for this is the enormous contribution from the recently arrived ring. (Leipper et. al., 1970, calculate a geostrophic transport of 40×10^6 m^3 s^{-1} associated with a young ring in August, 1965.

MONTH/ TRANSECT	REFERENCE LEVEL 400 m	600 m	1500 m
Jul 79			
from gyre center to western edge of current at 24°N	8.5[1]	9.9[1,2]	11.0[1,2]
from gyre center northwest along cruise trackline to edge of current	10.3[1]	12.8[1,2]	15.0[1,2]
Nov 79			
from gyre center to edge of current at 24°N	6.8[2]	8.3[2]	10.4[1,2]
from gyre center north - northeast to edge of current at 25°N	7.1	8.8	10.8[1,2]
Jul 80			
from gyre center to edge of current at 24°N	20.4[2]	22.4[2]	27.2[2]
from gyre center northwest along cruise trackline to edge of current	21.9	24.0	28.4[2]

1 Results include extrapolation of hydrographic data to depth.

2 Hydrographic data integrated up the bottom.

Table 2. Geostrophic transports X 10^6 m^3 s^{-1} along the transects indicated for July, 1979; November, 1979; and July, 1980 (see also the synoptic maps, Figures 4, 5, and 10).

Nowlin and Hubertz, 1979, calculate a geostrophic transport of 30×10^6 m^3 s^{-1} for a recently formed ring in June, 1967.

An intriguing question to ask is: If a ring arrives in the western Gulf just prior to the July, 1979, surveys, why do we not see the enhanced transport that we see in July, 1980? The USCGC Valiant XBT transect through the February, 1979, ring implies the ring has low amplitude; the change in depth of the 14°C isotherm across the ring is only 70 m. This ring may not noticeably enhance the pre-existing western Gulf circulation. However, this is a weak argument since it is based upon one transect only. Another possibility is that ring influence is advected well downstream by the pre-existing circulation by the time of the July, 1979, surveys. Advection of ring signal by mean flow in the western Gulf is shown in the next section.

Figures 12 and 13 show geostrophic velocity profiles across the western boundary current for July and November, 1979, and July, 1980. Figure 14 shows the geostrophic velocity profiles across the current for two segments of the July, 1979, west - east cruise trackline: the segment spanning the nearshore region of current concentration (see Figure 4) which is roughly 40 km wide; and the segment comprising the remaining 140 km of the trackline. Figures 12 - 14 show that, in general, the level of maximum vertical shear in the geostrophic velocity field occurs between the surface and 250 m. Using LORAN C to determine ship drift on the E-W section in July, 1979, surface drift reached 2 knots to the north. Figs. 12 - 14, of course show average values over the width of the flow.

2. Error Analysis - It is apparent from inspection of

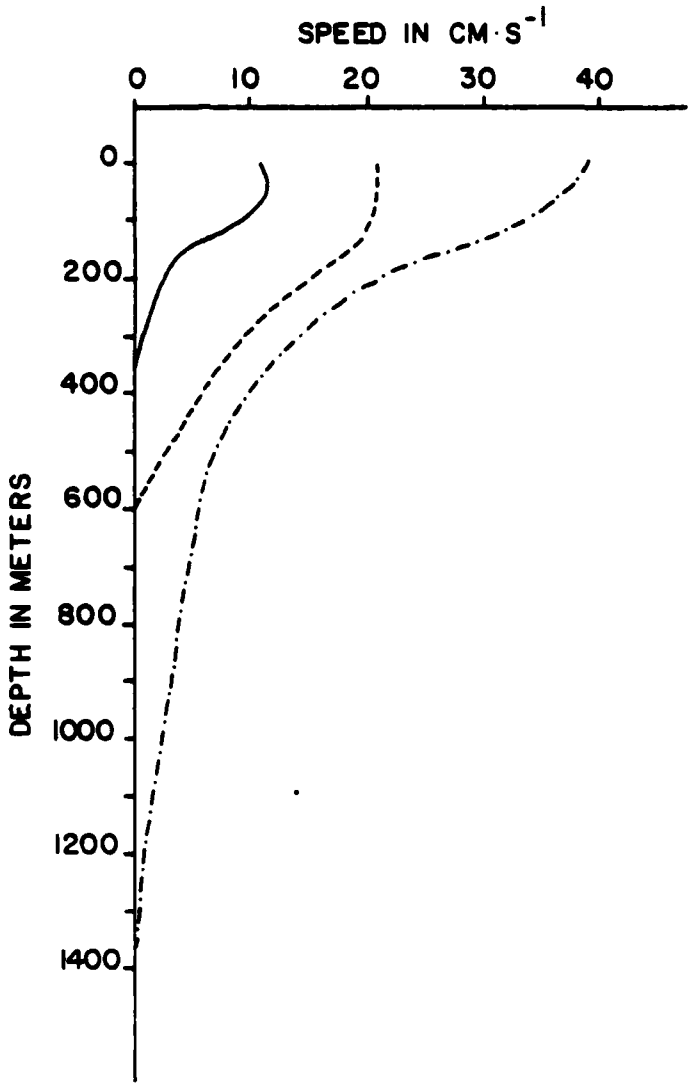

Figure 12. Geostrophic velocity versus depth across the western boundary current along west - east cruise tracklines:
——— July, 1979, relative to 400 m
----- November, 1979, relative to 600 m
—.— July, 1980, relative to 1500 m

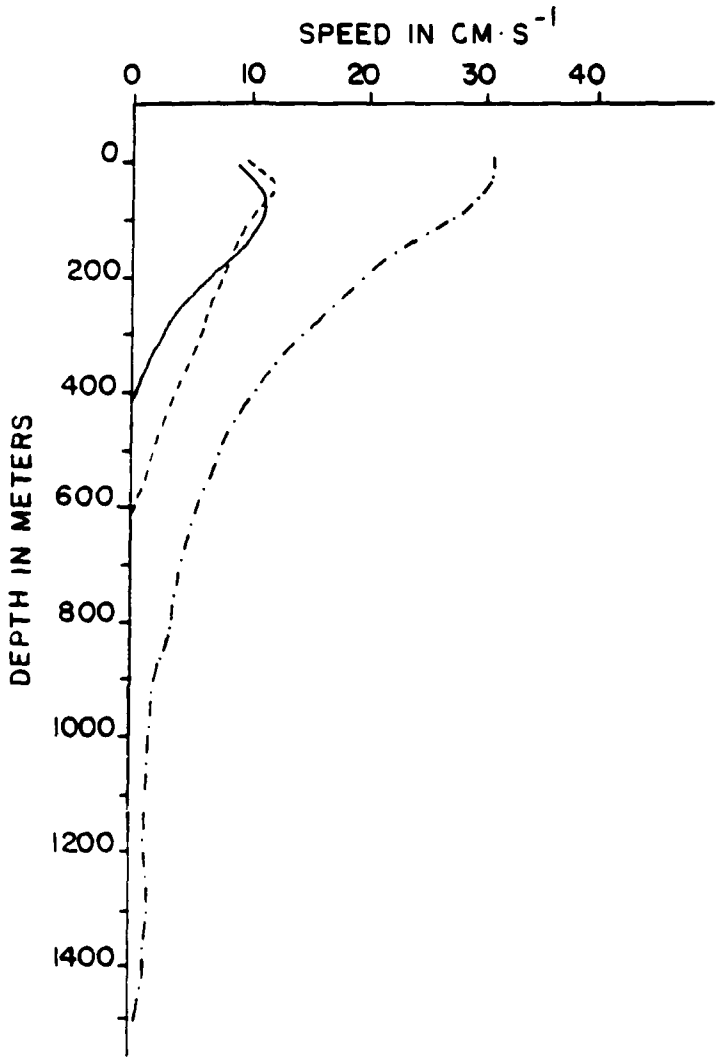

Figure 13. Geostrophic velocity versus depth across the western boundary current along southeast - northwest cruise tracklines (south - north for November):
——— July, 1979, relative to 400 m
----- November, 1979, relative to 600 m
—·— July, 1980, relative to 1500 m

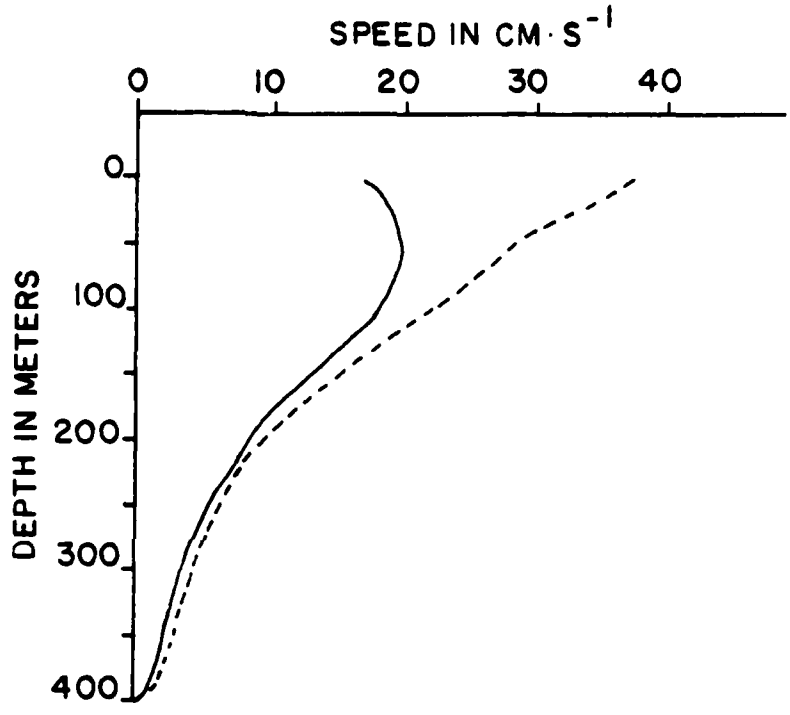

Figure 14. Geostrophic velocity versus depth relative to 400 m across the western boundary current along the west - east cruise trackline for July, 1979:
----- the first 40 km across the nearshore region of current concentration
——— the remaining 140 km. These values have been multiplied by five to facilitate comparison of the curves.

some of the vertical temperature sections that wave noise could be a significant error source (these vertical sections are shown later in Figures 19 and 20). Since the data showing waves extends to the 400 m depth only, the corresponding error is estimated for calculations referred to the 400 m level and the result generalized to the 1500 m level. The wave amplitudes vary from 5 - 80 m throughout the upper 400 m and intensify with depth as the stability increases. When the appropriate wave amplitudes are propagated throughout the transport calculations the error is at most on the order of 15% for July and November, 1979, and on the order of 5 - 10% for July, 1980. Salinities used in the calculations are determined from the cruise T - S curves. The maximum error introduced by transferring information off the T - S curves and by the accuracy of the salinity measurements is estimated to be 0.05 ppt, which results in transport errors of 3% in July and November, 1979, and of 1% in July, 1980. A temperature accuracy of $0.1^{o}C$ for XBT's and STD's and $0.3^{o}C$ for AXBT's results in maximum transport errors of 20% for July, 1979, 10% for November, 1979, and 5 - 10% for July, 1980. Warren and Volkmann (1968) calculate geostrophic transports across the Gulf Stream and conclude that significant error, ~20%, derives from an uncertainty in the positions and, therefore, exact hydrographic characteristics, of the edges of the current. In the present study, both the edge of the western boundary current and the gyre center are well sampled and well defined; a subjective estimate of the error due to inadequate edge and gyre center sampling is ± 5%. In July and November, 1979, where shallow

data are extrapolated to depth using historical data, additional errors of ± 5% (below 400 m) and ± 3% (below 600 m), respectively, result. Thus the transports in Table 2 are accurate to 26% for July, 1979; 19% for November, 1979; and 14% for July, 1980. When the error analysis is extended to the geostrophic velocities, the additional effect of uncertainty in position (.25 km for the loran c used) must be considered. This error is of the order of 1% or less and is considered negligible. Thus, the transport errors and velocity errors are essentially identical. The error analysis is summarized in Table 3.

Error introduced by:	% ERROR IN GEOSTROPHIC TRANSPORTS AND VELOCITIES FOR MONTH OF: Jul 79	Nov 79	Jul 80
wave noise	15%	15%	5 - 10%
salinity uncertainties	3%	1%	1%
temperature uncertainties	20%	10%	5 - 10%
edge and gyre center sampling uncertainties	5%	5%	5%
extrapolation of shallow data to depth using historical data	5%	3%	-
total error estimate:	26%	19%	~14%

Table 3. Summary of error estimates associated with the geostrophic calculation for: July, 1979; November, 1979; and July, 1980; assuming all error sources to be independent.

IV. INFLUENCE OF RINGS UPON THE BACKGROUND CIRCULATION

Based upon the analysis presented in the previous section, it is possible to observe influences of two rings upon the background circulation in the western Gulf during the period July, 1979 - June, 1980, using the method of Fourier decomposition.

A. Construction of the Time Series

Time series of the depth of the 14°C isotherm at various points in the western Gulf are constructed for the period July, 1979 - June, 1980. A smooth curve is fit by eye to the six available data points (July and November, 1979; February, March, May, June, 1980). The depth of the 14°C isotherm is picked off the curves at one month intervals, forming a twelve point series equally spaced in time. Figure 15 shows the time series at each point; their positions are indicated on Figure 16. The period of the dominant periodicity is on the order of six months.

There are two large gaps in the data sampling, one from July to October, 1979, and one from October, 1979, to February, 1980. The gaps do not necessarily result in severe loss of mesoscale information. When the current meter data available to date are used to "patch in" the July - November gap at points W and S (with positions corresponding

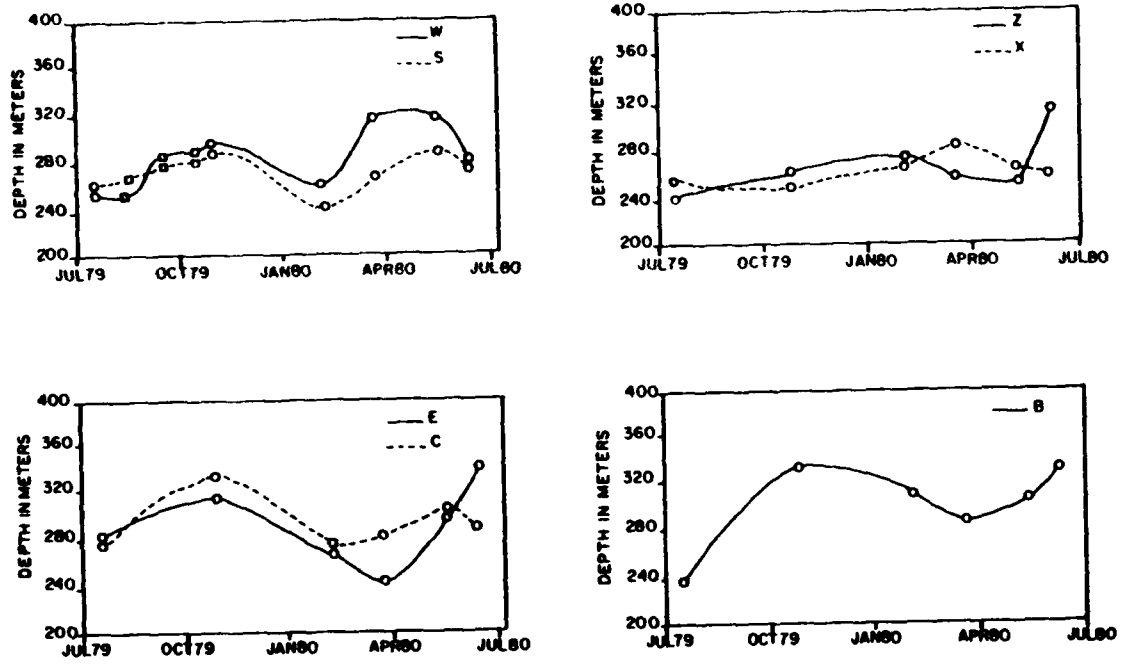

Figure 15. Time series of the depth of the 14°C isotherm at selected positions in the western Gulf of Mexico, July, 1979 - July, 1980. -o- from AXBT/cruise data; -●- from current meter mooring data. Positions are shown on Figure 16.

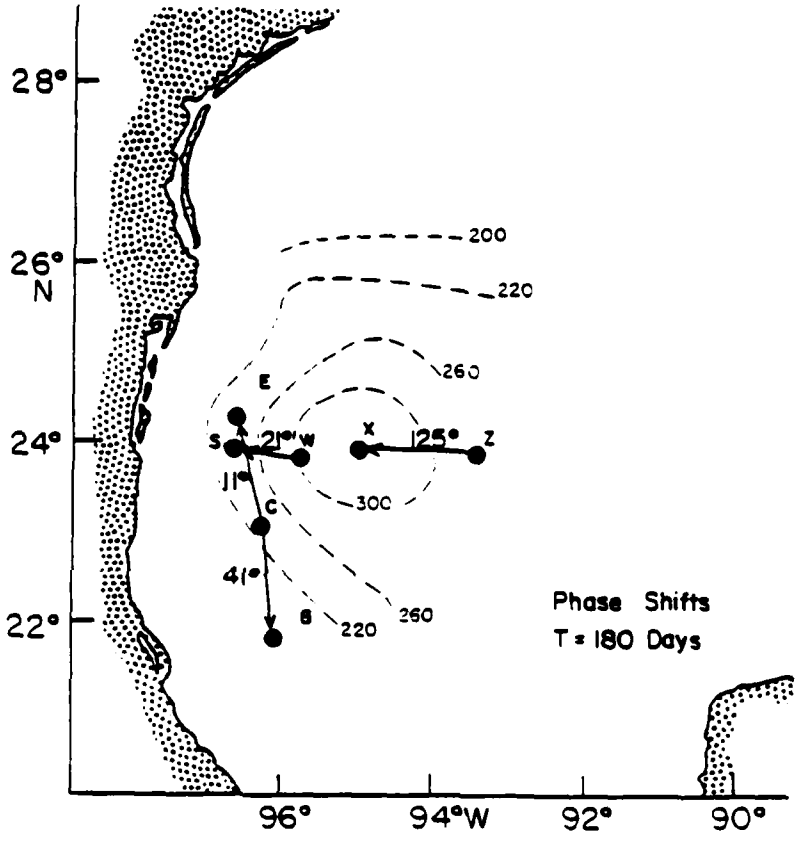

Figure 16. Phase shifts at six month periods between time series of depth of the 14°C isotherm in the western Gulf of Mexico. The dashed contours represent the mean depth of the 14°C isotherm during the period July, 1979 - July, 1980 (from Figure 11).

to current meter moorings), the basic character of the time series is not altered; see Figure 15.

B. Fourier Analysis

Figure 17 shows the autospectra at the seven points. The power consistently peaks at six months, in agreement with what we see in the time series. The six month period is interpreted as the length of time it takes ring signal to pass a point near the western Gulf boundary. The autospectra are only three band smoothed. The raw periodograms show lower power at the lowest frequency. Since the power peaks are only in the second spectral estimate, the time series are tapered 100% (see Bloomfield, 1976; his Figure 5.4).

It is usual practice to look at the position of a ring from one month to the next and compute the velocity of translation. Since the beginnings of a rudimentary time series exist, it is possible to attempt slightly improved calculations using the cross spectral method. Phase shifts for the period of interest (i.e. - six months), along with the corresponding coherence squared, phase confidence levels, and error estimates are shown in Table 4. Confidence levels are low because the 100% tapering is used, requiring a corresponding reduction in the number of effective degrees of freedom.

Although the body of data is large enough in space and time to

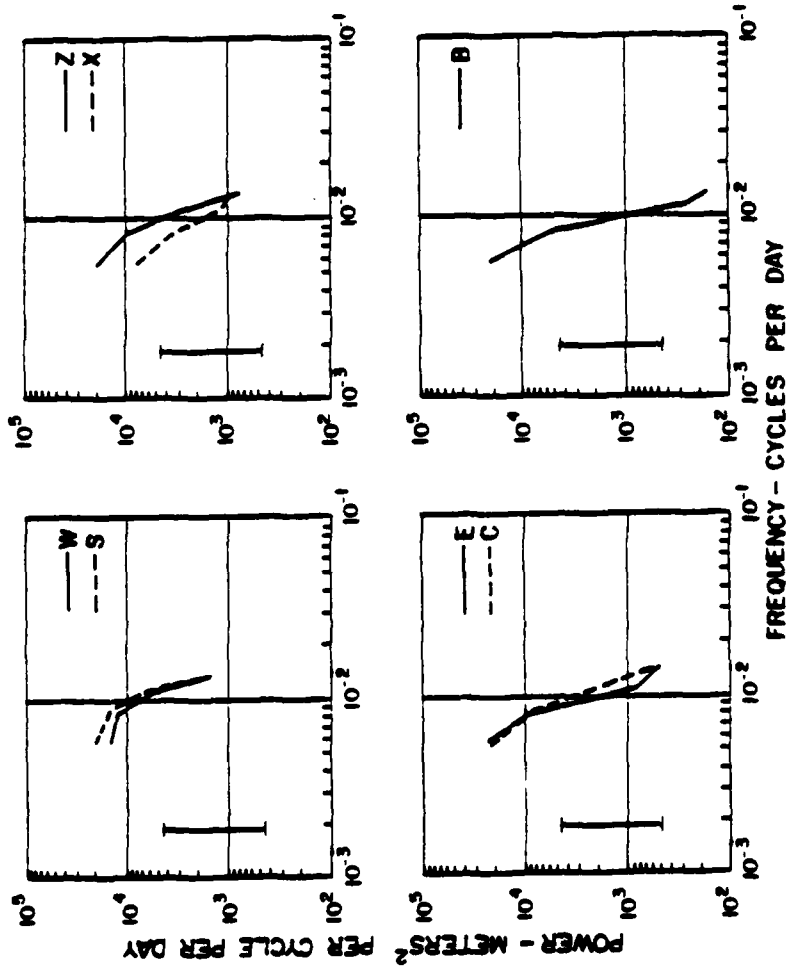

Figure 17. Autospectra of the depth of the 14°C isotherm at the locations indicated (see Figure 16). Time series are tapered 100%. Spectra are three band smoothed.

CROSS SPECTRA	PHASE SHIFT	(COHERENCE)^2	CONFIDENCE LEVEL	PHASE SHIFT ERROR ESTIMATE
Z to X	125^{o}	.95	80%	10^{o}
W to S	21^{o}	.84	60%	12^{o}
C to E	11^{o}	.81	60%	13^{o}
C to B	41^{o}	.84	60%	12^{o}

Table 4. Coherence squared, confidence levels, and error estimates for phase shift calculations (see text and Figure 17).

permit decomposition of the signal into its Fourier components, the results are representative only for the two rings actually seen. The high degree of statistical confidence associated with long records is absent; however, the calculations of phase shift are entirely valid for this realization.

C. Interpretation of Phase

The phase shifts directed onshore are associated with ring influx. A wavelength of 426 km is calculated from the 125° phase shift between points Z and X, the two most offshore points which are located in deep water (the remainder of the points in Figure 16 are located in shoaling water). This wavelength is roughly 30% greater than the east - west length scale and is comparable to the north - south length scale of the May warm core ring, Figure 8; Table 1B.

A dispersion curve for first vertical mode baroclinic Rossby waves in the Gulf of Mexico using the Rhines (1977) linear, quasi-geostrophic, β - plane model for an ocean of constant stratification is constructed, and is shown in Figure 18. Input parameters are:

typical wavelength - 430 km (from Z to X phase shift)

basin north to south bottom slope - 3 m/km down to the south

internal Rossby radius of deformation - 120 km

typical basin depth - 3 km.

Also shown on Figure 18 is the point in wavelength/period space derived from the Z to X 125° phase shift. The constant stratification model provides a fairly good match to the data.

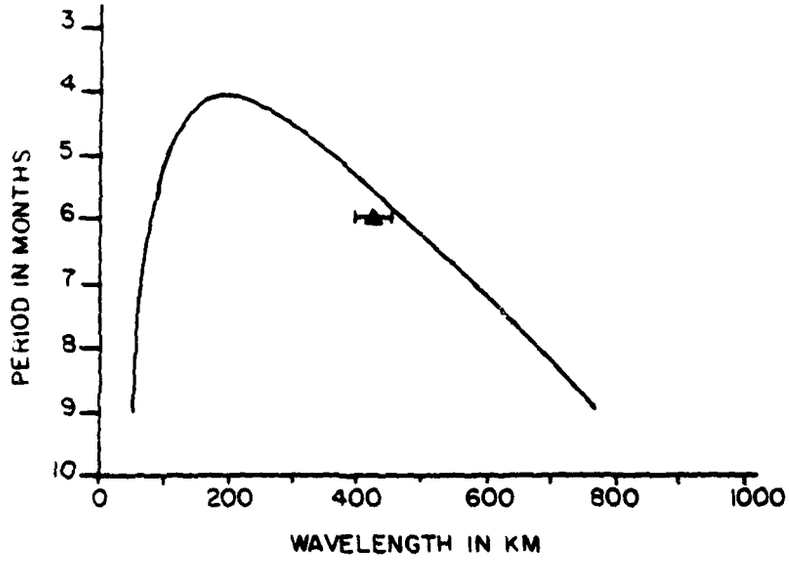

Figure 18. Dispersion curve for first vertical mode baroclinic Rossby waves in the Gulf of Mexico, calculated using the Rhines (1977) model. Data point is derived from the Z to X phase shift at six month periods.

If it is assumed that a ring behaves similarly to a first vertical mode baroclinic Rossby wave, then Figure 18 suggests that if some part of the incoming energy is reflected by the continental slope and/or rise, the reflected signal at six-month periods has a wavelength of about 80 km. Figure 19 is a vertical temperature section along 24°N. The wavelengths on the order of 70 - 80 km are suggestive of reflection of ring energy by the western boundary. Figure 20 is a vertical temperature section along trackline 2 of the R.V. Longhorn cruise in July, 1980 (see Figure 10). Again, the wavelengths on the order of 70 - 80 km suggest reflection of ring energy by the western boundary. The agreement between the observations and the model seems quite meaningful. The wave amplitude of the reflected signal at the 14°C isothermal surface (~45 m in July, 1979, and ~79 m in July, 1980) is less than that of the incoming signal (of ~70 m in February, 1979, and ~123 m in March, 1980).

The purpose of the "fit" of our data to the dispersion curve shown in Fig. 18 is to allow us to ask what might be the wavelength of reflected energy, if it is not all swept away by the western boundary current. There is a considerable body of opinion, however, that a pinched-off ring is dynamically dissimilar to a free Rossby wave (e.g., Nof, 1981), so we view the fit of Fig. 18 with caution.

The southward directed phase may be interpreted to represent topographically trapped waves propagating along the continental rise.

The northward directed phase suggests the advection of phase by mean flow. The group velocity and phase speed associated with the incoming ring energy are 2 and 3 cm s^{-1}, respectively; while the geostrophic velocity profiles (e.g. - see Figure 12) imply a steering velocity on the order of 10 cm s^{-1}.

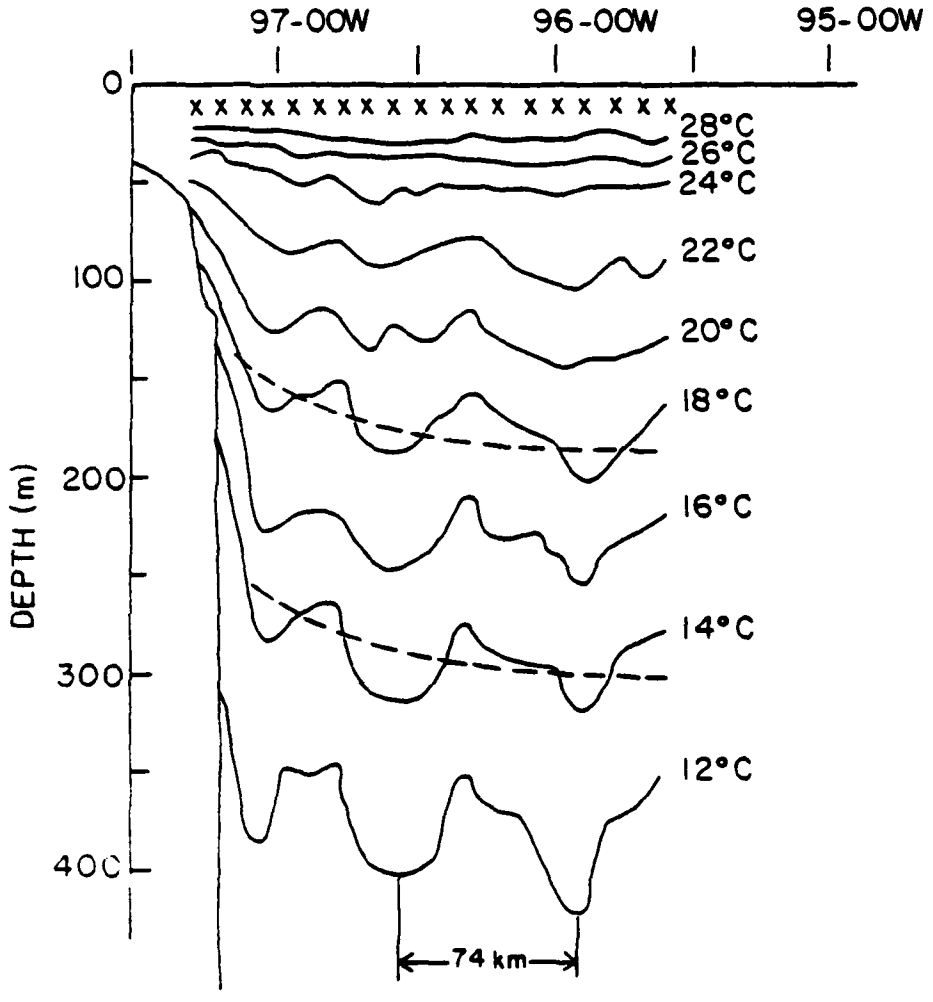

Figure 19. Vertical temperature section along 24°N from R.V. Longhorn cruise, July, 1979. The wavelength of the wave feature is about 74 km. Dashed contours represent the general downward offshore slope of the isotherms which is associated with the western boundary current. X's indicate ship XBT drops.

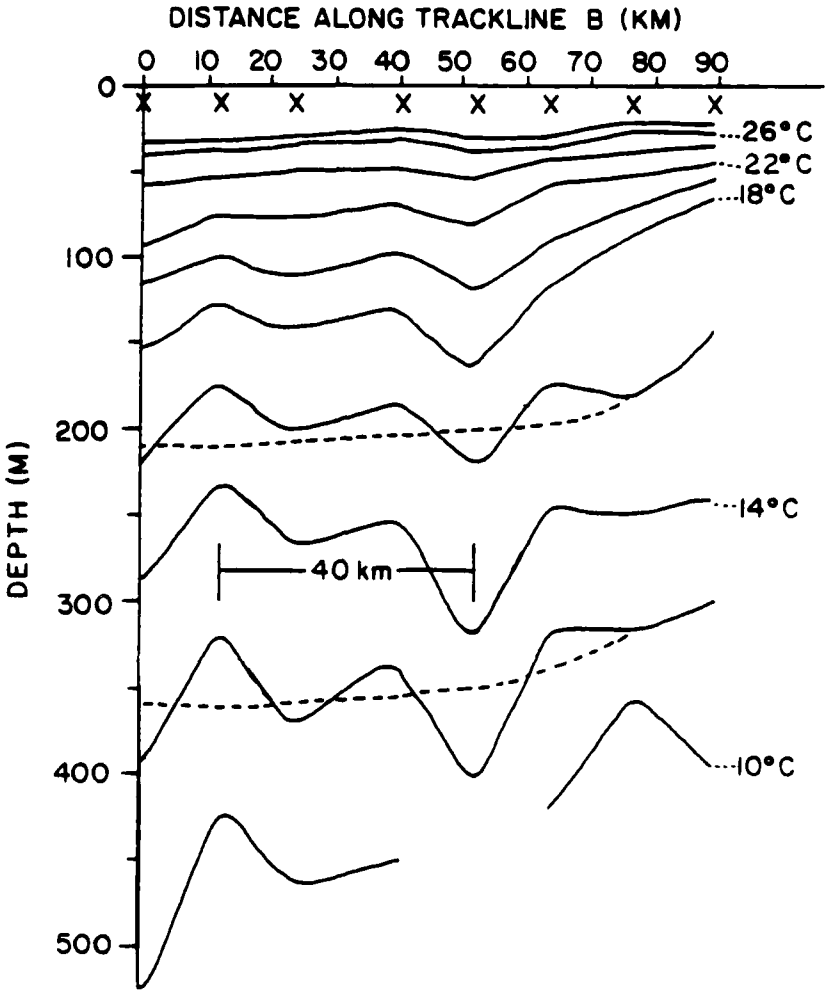

Figure 20. Vertical temperature section along trackline 2 of R.V. Longhorn cruise, July, 1980; see Figure 10. The half wavelength of the wave feature is about 40 km. Dashed contours represent the general downward offshore slope of the isotherms which is associated with the western boundary current. X's indicate ship XBT drops.

V. HORIZONTAL WAVE NUMBER SPECTRA

Figure 21 shows mean spectral estimates for zonal and meridional spatial series of the depth of the 14°C isotherm derived from ship XBT transects. The wave number spectra are not significantly different between wavelengths of 200 km and 50 km, falling off as $\sim k^{-3}$. However, the zonal power at the Nyquist is larger by a factor of four. There is no reason for a higher instrumental noise level zonally. There must be greater aliasing at the shorter wavelengths zonally than meridionally, largely because the east - west transects approach the coast, while the north - south transects lie more offshore. The internal wave signal is greater in regions of strong bottom slope.

The bulk of the data used in the Fourier analysis of the previous section is derived from the AXBT flights. As previously discussed, temporal aliasing is not considered a problem of great import. The possible effects of spatial aliasing also prove to be unimportant. An estimate of the AXBT mean east - west drop spacing is 45 km. Thus the sampling interval is not expected to permit consistent resolution of wavelengths on the order of those associated with reflection of ring energy; 80 km wavelengths alias to wavelengths of 150 km and greater. Since the ship zonal wave number spectra are "red" out to wavelengths of 50 km, it is unlikely that aliasing will significantly bias the

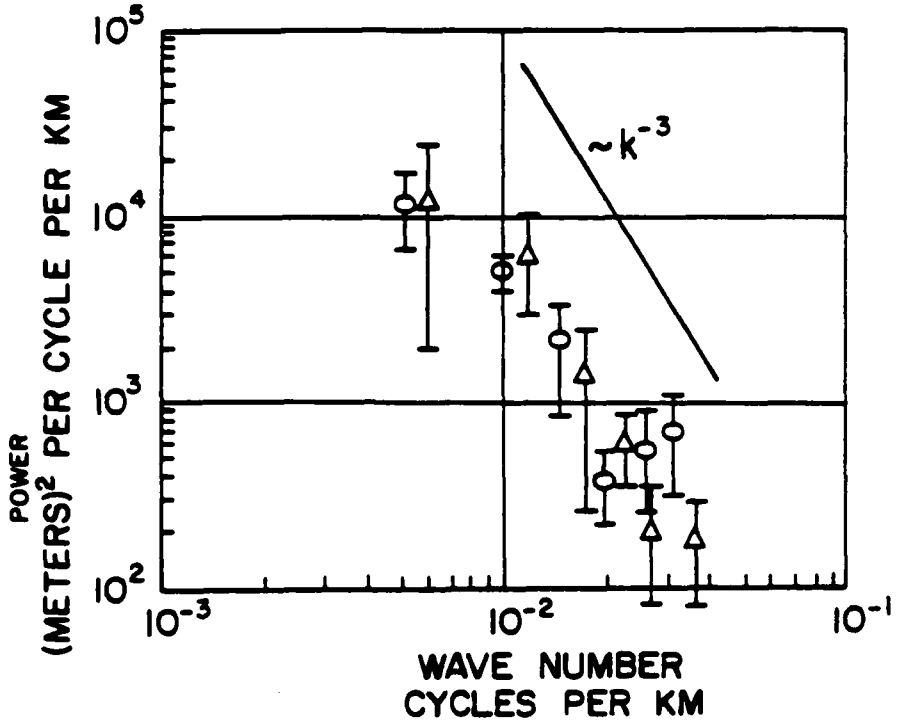

Figure 21. Cruise horizontal wave number spectra. Shown are mean spectral estimates for the depth of the 14°C isotherm in the western Gulf of Mexico.
-o- along 24°N, from July, 1979; November, 1979; and July, 1980.
-Δ- along 95°-30'W, from July, 1979, and November, 1979; along 95°W and 94°W from July, 1980. These estimates are for the same wave numbers as in -o-, but are offset slightly to the right.
Each spatial series is tapered 100%. Error bars are one standard deviation.

results or interpretation in the zonal sense. The AXBT north - south drop spacing varies much more than the east - west spacing, ranging from 40 km to 100 km. Yet, it is unlikely that spatial aliasing in the north - south sense will introduce significant bias since the average meridional spectrum is "red" out to the Nyquist. To summarize, since the power is low at wavelengths of 50 - 100 km, and since the wave number spectra are "red", a "poor" AXBT drop spacing may be utilized, permitting the sampling of longer transects.

Figure 22 shows mean spectral estimates for spatial series of the depth of the $14^{o}C$ isotherm, which are derived from the lower resolution AXBT surveys. The greatest power lies, as expected, at wavelengths of 250 km - 500 km, with power then falling off as $\sim k^{-3}$ or greater. This is consistent with what is already known; the length scales of the dominant mesoscale eddies are on the order of a few hundred kilometers. If the high wave number ends of the spectra in Figure 22 are attached to the low wave number ends of the corresponding spectra in Figure 21 (this is done in Figure 23 for the zonal spectra along $24^{o}N$) the two, which are independently calculated, overlap nicely and form continuously "red" spectra. The power fall off trends ($\sim k^{-3}$) in these Gulf of Mexico wave number spectra are consistent with what is observed in the North Atlantic (see Sturges and Summy, 1981; their Figure 11) and in the North Pacific (see Wilson and Dugan, 1978; their Figure 4).

An estimate of the noise level associated with an AXBT may be calculated from the wave number spectra of Figure 22. Assuming the spectral estimate at the highest wave number is representative of

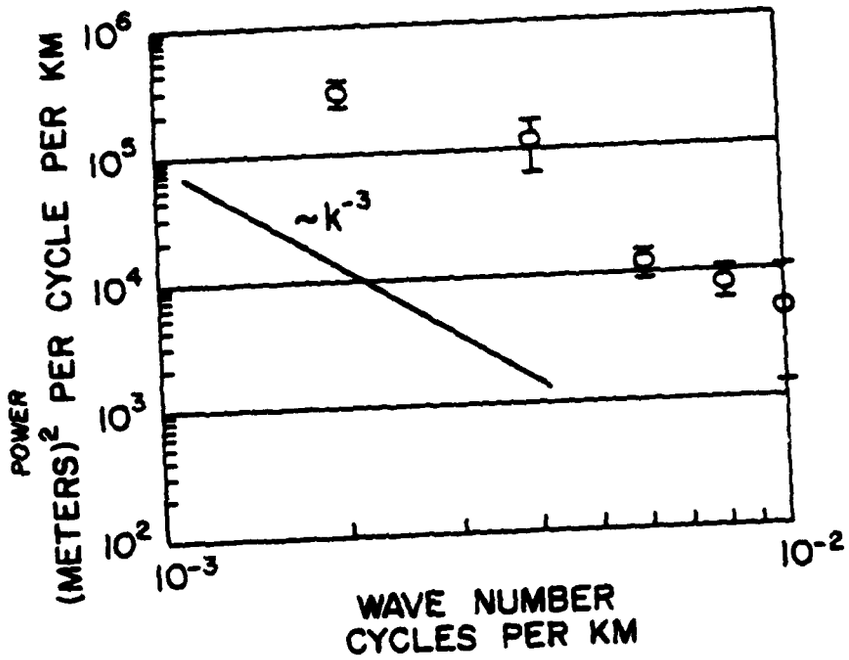

Figure 22A. AXBT horizontal wave number spectra. Shown are mean spectral estimates for the depth of the 14°C isotherm in the western Gulf of Mexico along 24°N, from July, 1979; May, 1980; and June, 1980. Each spatial series is tapered 100%. Error bars are one standard deviation.

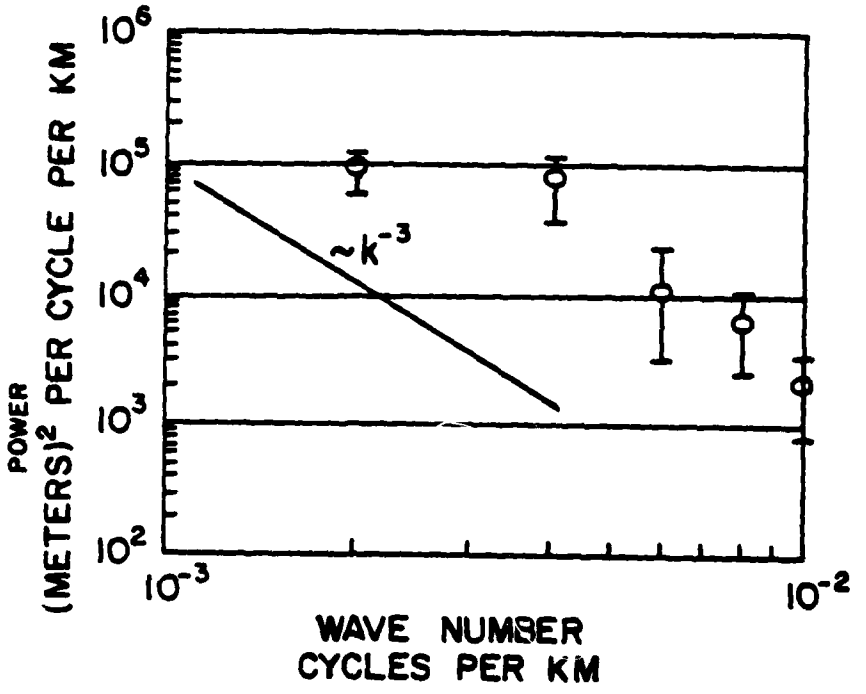

Figure 22B. Same as Figure 22A, but along 25°N, from November, 1979; May, 1980; and June, 1980.

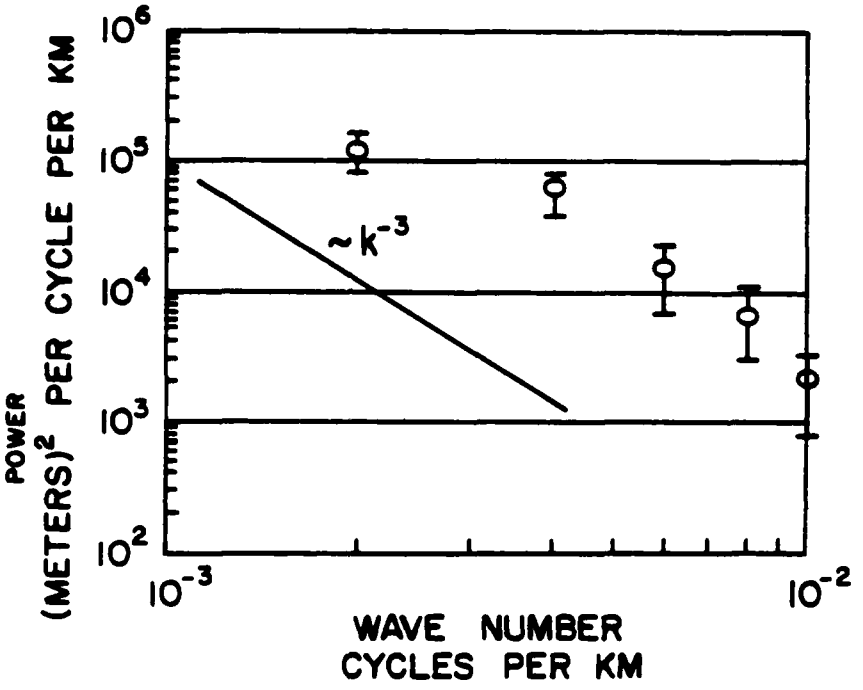

Figure 22C. Same as Figure 22A, but along 95°W, from February, 1980; and March, 1980; and along 95°-30'W, from May, 1980; and June, 1980.

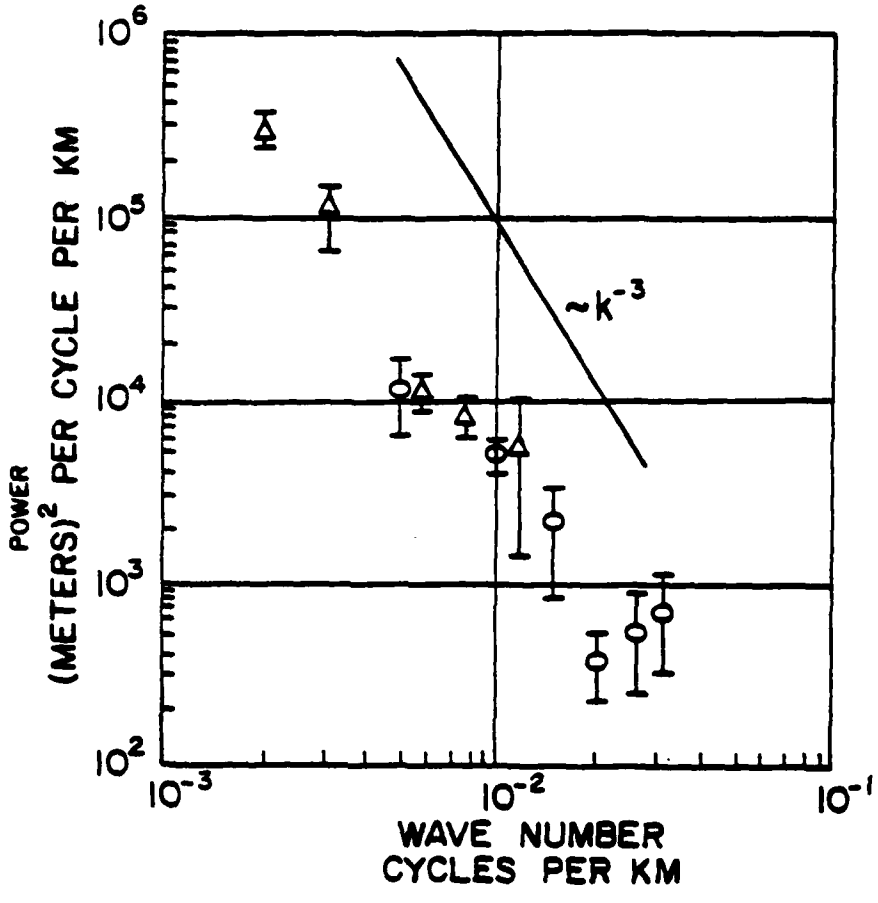

Figure 23. Composite plot of horizontal wave number mean spectral estimates along 24°N. -o- from cruises (Figure 21). -Δ_2 from AXBT flights (Figure 22); the estimate at wave number 10^{-2} is offset slightly to the right.

the noise level, a variance of ~28 m^2 is calculated, implying a noise level of ~5 m. This agrees with the subjective estimate of 5 - 10 m presented earlier.

CONCLUSIONS

The background circulation in the central and western Gulf has superimposed upon it the influence of the warm core anticyclonic rings which separate from the Loop Current at an average period of nine to ten months and generally translate westward across the basin. The background circulation presumably is forced by the curl of the wind stress, which, in this region, is predominantly negative throughout the year. The basin is expected to respond with a Sverdrup interior in the mean, provided the β and curl terms dominate the mesoscale eddy terms in the vorticity balance; and, in the time dependent sense, with either time varying Sverdrup flow or the production of Rossby waves. Mean interior southerly flow is calculated via two independent methods. The Sverdrup relation gives a transport of 5.6×10^6 m^3 s^{-1}; while the geostrophic calculation yields transport relative to 1500 m of 8.5×10^6 m^3 s^{-1}. That it is possible to calculate interior flow to the south using historical data seems a convincing result and may be considered as evidence for wind stress curl forcing.

Associated with the background interior circulation is a western boundary current return flow. Geostrophic transport relative to 1500 m of at least 10×10^6 m^3 s^{-1} is calculated for this current. The current typically flows along the western boundary north of 22^oN and

turns offshore in the vicinity of 25°N to 26°N, beyond which extensive meandering and possibly even ring separation may occur. At times, the flow associated with the offshore limb may be supplemented by shelf derived flow from the north. The level of maximum vertical shear in the geostrophic velocity field occurs between the surface and 250 m.

This data set suggests that incoming rings can interact with the western Gulf gyre in a wave-like manner. Some of the ring energy incident upon the western boundary is reflected at shorter wavelengths, consistent with Rossby wave theory, and some propagates south along the continental rise in the form of topographically trapped waves. Additionally, the incoming, reflected, and southward propagating signals may be advected by the western boundary current north of 23°N. The interior geostrophic transport calculation shows that ring signal greatly dominates the background signal in the interior. This can also be true in the western Gulf; geostrophic transports in July, 1980, across the western boundary current are greatly enhanced by the ring which arrived in June.

ACKNOWLEDGEMENTS

This research was sponsored by the Office of Naval Research under contract #N00014-75-C-0201 and the National Science Foundation under contract #OCE-7820722.

One of the authors (Mr. Rick Kassler) was supported by the U.S. Coast Guard post-graduate training program.

We wish to acknowledge the work of Patrol Squadron VP 94, U.S. Naval Reserve, operating out of New Orleans, La., that made possible the AXBT maps, and LCDR John Roeder, USN, who made the logistics work out.

We thank the crew of the R/V Longhorn, Don Gibson, master, for their enthusiastic cooperation during several cruises, and also the crew of the R/V Iselin for their able assistance.

We thank Mr. J.C. Evans for his computer programming, and Ms. Patty Arnold and Ms. Jill Kuhlman for typing and other help.

LIST OF REFERENCES

Behringer, David W., Robert L. Molinari, and John F. Festa, (1977), The Variability of Anticyclonic Current Patterns in the Gulf of Mexico. J. Geophys. Res., 82, 34, 5469-5476.

Blaha, John P. and Wilton Sturges, (1978), Evidence for Wind Forced Circulation in the Gulf of Mexico. Technical Report. The Florida State University, Department of Oceanography, Tallahassee, Florida, 134 pp.

_____, (1981), Evidence for Wind Forced Circulation in the Western Gulf of Mexico. J. Mar. Res., in press.

Bloomfield, Peter, (1976), Fourier Analysis of Time Series, An Introduction. John Wiley and Sons Inc., New York, New York, 258 pp.

Clemente-Colon, Pablo, (1980), On the Circulation Processes of the Western/Northwestern Gulf of Mexico: A Satellite and Hydrographic View. M.S. Thesis. Texas A & M University, College Station, Texas, 126 pp.

Cochrane, John D., (1972), Separation of an Anticyclone and Subsequent Developments in the Loop Current (1969). In Contributions on the

Physical Oceanography of the Gulf of Mexico, Texas A & M University Oceanographic Studies, Volume 2. Gulf Publishing, Houston, Texas, 91 - 106.

Elliott, Brady Alan, (1981), Anticyclonic Rings in the Gulf of Mexico. Manuscript submitted to J. Phys. Oceanogr.

Emery, K. O. and G. T. Csanady, (1973), Surface Circulation of Lakes and Nearly Land-Locked Seas. Proc. Nat. Acad. Sci. USA., 70, 1, 93 - 97.

Flierl, Glenn R., (1977), The Application of Linear Quasigeostrophic Dynamics to Gulf Stream Rings. J. Phys. Oceanogr., 7, 5, 365 - 379.

Harrison, D. E., (1979), The Importance of Length Scales on Variation of Eddy Statistics. Polymode News, No. 62. (unpublished manuscript).

Hastenrath, Stephan and Peter J. Lamb, (1977), Climatic Atlas of the Tropical Atlantic and Eastern Tropical Pacific Oceans. University of Wisconsin Press, Madison, Wisconsin.

Hellerman, S., (1967), An Updated Estimate of the Wind Stress on the World Ocean. Mon. Weather Rev., 95, 9, 607 - 626; see also correction, ibid., 96, 1, 63 - 74.

Hurlburt, H. E. and Dana Thompson, (1980), A Numerical Study of Loop Current Intrusions and Eddy Shedding. J. Phys. Oceanogr., 10,

1611 - 1651.

Ichye, T., (1962), Circulation and Water Mass Distribution in the Gulf of Mexico. Geofisica International, 2, 47 - 76.

Krishnamurti, T. N. and R. Krishnamurti, (1979), Surface Meteorology of the A-Scale during One-Hundred Days of Gate. Deep Sea Res., Gate Supplement II to 26, 29 - 62.

Leetmaa, Ants, Pearn Niiler, and Henry Stommel, (1977), Does the Sverdrup Relation Account for the Mid-Atlantic Circulation? J. Mar. Res., 35, 1, 1 - 10.

Leipper, D. F., J. D. Cochrane, and LCDR J. F. Hewitt, USN, (1972), A Detached Eddy and Subsequent Changes (1965). In Contributions on the Physical Oceanography of the Gulf of Mexico, Texas A & M University Oceanographic Studies, Volume 2. Gulf Publishing, Houston, Texas, 107 - 118.

Lindstrom, Eric J., David W. Behringer, Bruce A. Taft, and Curtis C. Ebbesmeyer, (1980), Absolute Geostrophic Velocity Determination from Historical Hydrographic Data in the Western North Atlantic. J. Phys. Oceanogr., 10, 7, 999 - 1009.

McLellan, Hugh J. and Worth D. Nowlin, (1962), The Waters of the Gulf of Mexico as Observed in February and March 1962. Data Report. Texas A & M University, College Station, Texas.

McWilliams, James C. and Glenn R. Flierl, (1979), On the Evolution of Isolated, Nonlinear Vortices. J. Phys. Oceanogr., 9, 11, 1155 - 1182.

Merrell, William J., Jr. and John M. Morrison, (1981), On the Circulation of the Western Gulf of Mexico with Observations from April, 1978. J. Geophys. Res., 86, C5, 4181 - 4185.

Molinari, Robert L., (1978), The Relationship of the Curl of the Local Wind Stress to the Circulation of the Cayman Sea and the Gulf of Mexico. J. Phys. Oceanogr., 8, 5, 779 - 784.

_____, (1980), Current Variability and Its Relation to Sea-Surface Topography in the Caribbean Sea and Gulf of Mexico. Mar. Geodesy, 3, 409 - 436.

Nof, Doron, (1981), On the β-induced Movement of Isolated Baroclinic Eddies. J. Phys. Oceanogr., in press.

Nowlin, W. D. Jr., (1972), Winter Circulation Patterns and Property Distributions. In Contributions on the Physical Oceanography of the Gulf of Mexico, Texas A & M University Oceanographic Studies, Volume 2. Gulf Publishing, Houston, Texas, 3 - 53.

_____ and J. M. Hubertz, (1972), Contrasting Summer Circulation Patterns for the Eastern Gulf-Loop Current Versus Anticyclonic Rings. In Contributions of the Physical Oceanography of the Gulf of Mexico, Texas A & M University Oceanographic Studies, Volume 2. Gulf Publishing, Houston, Texas, 119 - 138.

_____ and H. J. McLellan, (1967), A Characterization of

the Gulf of Mexico Water in Winter. J. Mar. Res., 25, 1, 29 - 59.

Rhines, Peter B., (1977), The Dynamics of Unsteady Currents. In The Sea, Vol. VI. John Wiley and Sons, New York, New York, 189 - 318.

Stommel, Henry, (1964), Summary Charts of the Mean Dymanic Topography and Current Field at the Surface of the Ocean and Related Functions of the Mean Wind Stress. In Studies on Oceanography. University of Washington Press, Seattle, Washington.

Stroup, Edward D., Bernard J. Kilonsky, and Klaus Wyrtki, (1981), AXBT Observations During the Hawaii/Tahiti Shuttle Experiments. Technical Report. The University of Hawaii, Honolulu, Hawaii.

Sturges, Wilton and John P. Blaha, (1976), A Western Boundary Current in the Gulf of Mexico. Science, 192, 367 - 369.

_____ and Alan Summy, (1981), Low-Frequency Temperature Fluctuations Between Ocean Station Echo and Bermuda. Manuscript submitted to J. Mar. Res.

Vukovich, Fred M., Bobby W. Crissman, Mark Bushnell, and William J. King, (1979), Some Aspects of the Oceanography of the Gulf of Mexico Using Satellite and In Situ Data. J. Geophys. Res., 84, C12, 7749 - 7768.

Warren, Bruce A. and G. H. Volkmann, (1968), Measurement of Volume Transport of the Gulf Stream South of New England. J. Mar. Res.,

26, 2, 110 - 126.

Wilson, W. S. and J. P. Dugan, (1978), Mesoscale Thermal Variability in the Vicinity of the Kuroshio Extension. J. Phys. Oceanogr., 8, 537 - 540.

Appendix A - Additional figures

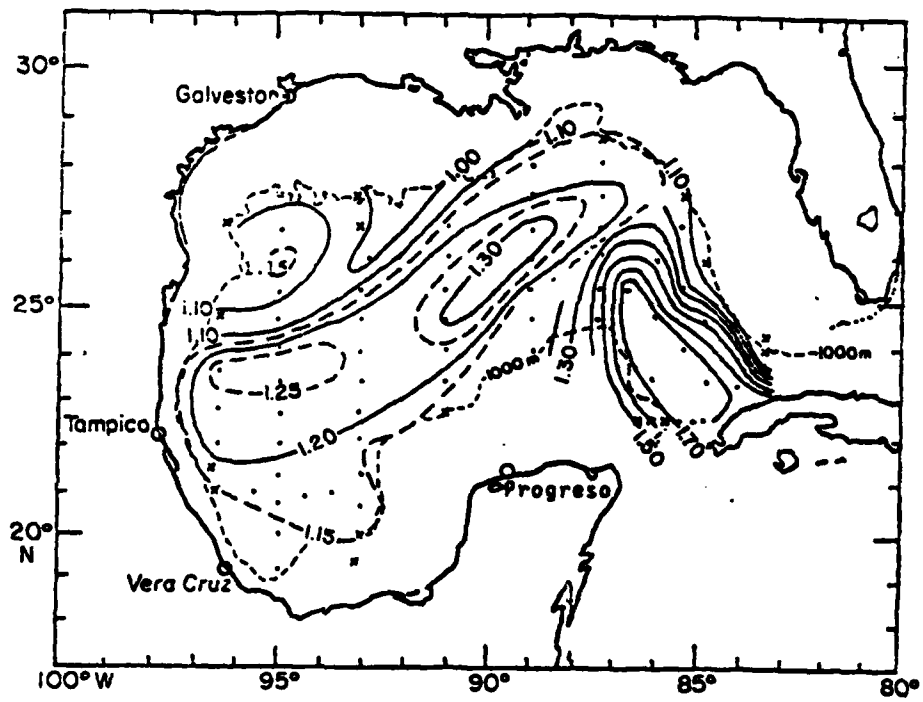

Figure A-1. "An adaptation of Figure 1-29 from Nowlin, 1972 (also of Figure 20 from Nowlin and McLellan, 1967): 'Dynamic topography of sea surface relative to the 1000-db surface, Hidalgo 62-H-3; X's indicate some extrapolation. Contour interval 0.05 dynamic meters.' The very strong feature in the lower right is associated with the Loop Current."

Caption and figure from Blaha and Sturges (1978).

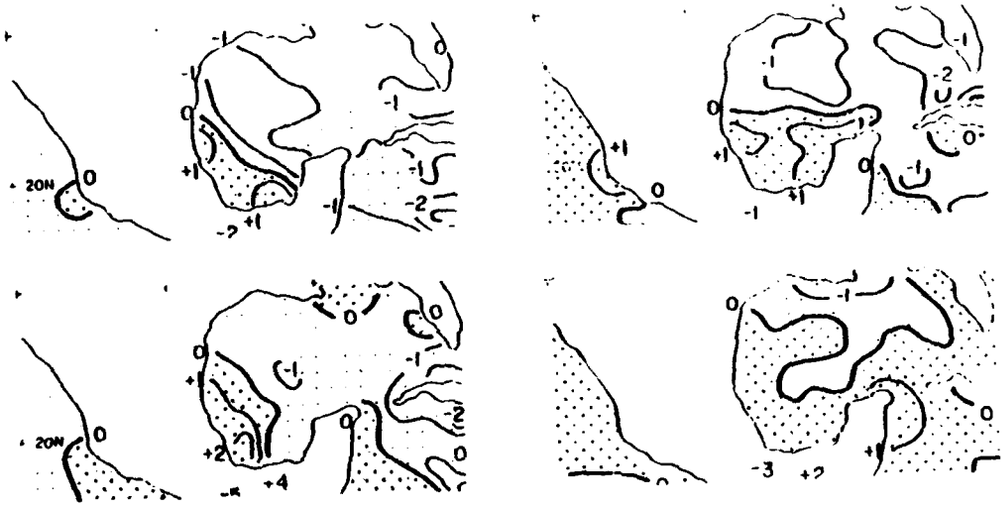

Figure A-2. Mean wind stress curl X 10^{-8} dynes cm^{-3}, 1911 - 1970, contoured by 1^{o} squares for (clockwise from top left) January, April, October, and July. From Hastenrath and Lamb (1977), their charts 46 - 49.

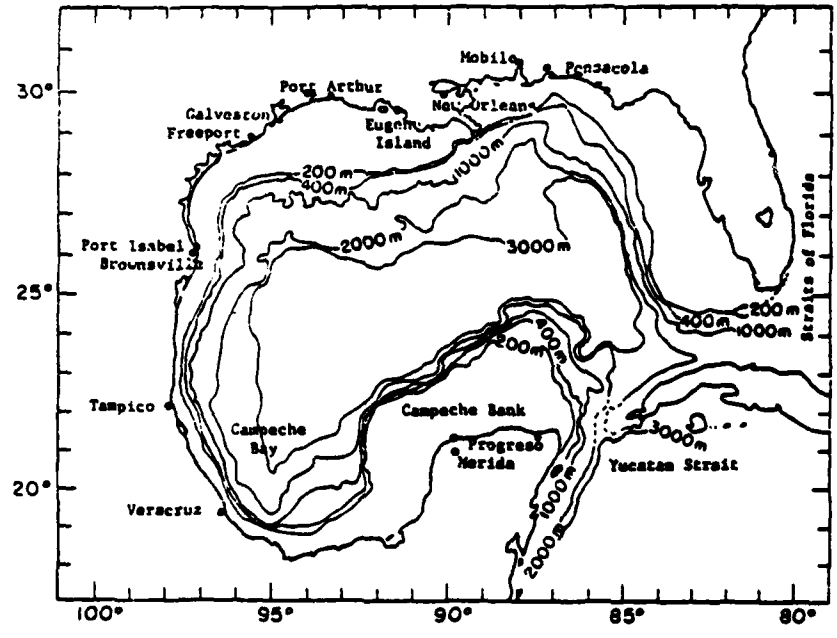

Figure A-3. Bathymetry in the Gulf of Mexico, from Nowlin (1972), Figure 1 - 2.

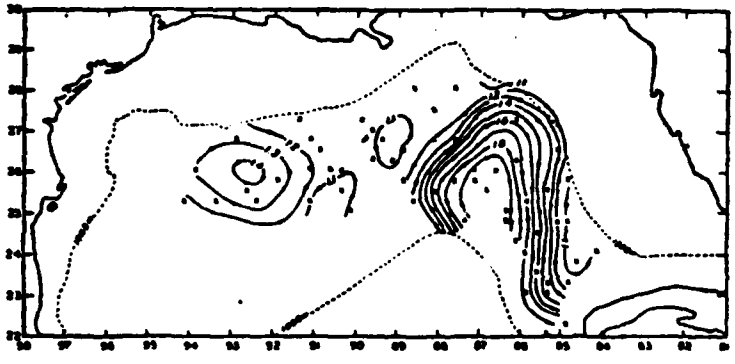

Figure A-4. Dynamic topography of the sea surface relative to the 1000-db surface for 14 August - 4 September, 1968, from Figure 8, Molinari (1980). Maps such as these were used in determining positions and characteristics of hydrostations located in regions unaffected by Loop Current and ring presence.

Appendix B - Estimation of mean annual Ekman transport

Mean annual surface wind velocity, $\vec{V}$, across Gulf deep basin at 25^{o} N: 350 cm s^{-1} at ~ 270^{o} T (Hastenrath and Lamb, 1977)

Surface wind stress $\vec{\tau} = \rho_a C_d |\vec{V}| \vec{V}$

where $\rho_a \equiv$ density of air = 1.2×10^{-3} g cm^{-3}

$C_d \equiv$ drag coefficient = 1.3×10^{-3}

$\therefore \vec{\tau}$ = 0.19 g cm^{-1} s^{-2} to the west

Ekman mass transport $\vec{M^E} = \frac{\tau \times k}{f}$

where $f \equiv$ Coriolis parameter = 6×10^{-5} s^{-1}

$\therefore \vec{M^E} = 3.19 \times 10^{3}$ g $cm^{-1} s^{-1}$ to the north

Ekman volume transport $\vec{V^E} = \vec{M^E} L \alpha$

where $L \equiv$ applicable east - west basin extent = 700 km

$\alpha \equiv$ specific volume of sea water $\cong$ 1 cm^3 g^{-1}

$\therefore \vec{V^E} = 0.2 \times 10^{6}$ m^3 s^{-1} to the north

Appendix C - Estimation of mean annual interior geostrophic transport

Background dymanic height relative to 1000 m in eastern Gulf:

$1.05\ m^2\ s^{-2}$ (from original calculation, see text pp. 8 - 14)

Dynamic height relative to 1000 m in western Gulf:

$1.34\ m^2\ s^{-2}$ (from original calculation, see text pp. 8 - 14)

rms diameter of a ring in eastern Gulf:

370 km (Elliott, 1981)

Mean translational speed of a ring:

$3\ km\ day^{-1}$ (Elliott, 1981)

Therefore, time for ring to pass a point in eastern Gulf:

$\frac{1}{3}$ year

Dynamic height relative to 1000 m at center of a ring in eastern Gulf:

$1.80\ m^2\ s^{-2}$ (Molinari, 1980; Figure 8)

Assume ring pinch off period of one year.

Assume ring is like a cosine perturbation superimposed upon background signal.

Then average dynamic height relative to 1000 m across a ring, $\overline{R(X)}$, is:

$$1.05 + \frac{0.75}{\pi} \int_{\frac{-\pi}{2}}^{\frac{\pi}{2}} \cos x \, dx$$

$$\overline{R(X)} = 1.5275 \ m^2 \ s^{-2}$$

$\overline{R(X)}$ acts on a typical point in the eastern Gulf for $\frac{1}{3}$ of the year. Thus, the annual average dynamic height relative to 1000 m at a typical point in the eastern Gulf, $\overline{D(X)}$, is

$$\frac{(1.05 \times 2) + \overline{R(X)}}{3} = 1.2092 \ m^2 \ s^{-2}$$

The interior geostrophic transport calculation yields $19 \times 10^6 \ m^3 \ s^{-1}$ to the south. Now, forming a ratio:

$$\frac{(1.34 - 1.05) \ m^2 \ s^{-2}}{19 \times 10^6 \ m^3 \ s^{-1}} = \frac{(1.34 - 1.21) \ m^2 \ s^{-2}}{Y \times 10^6 \ m^3 \ s^{-1}}$$

$$Y = 8.5 \times 10^6 \ m^3 \ s^{-1}$$

where Y is the estimate of mean annual geostrophic flow to the south.